Novel Organic Light Emitting Diodes for Optogenetic Experiments

by

Ankur Shah

A Thesis Presented in Partial Fulfillment
of the Requirements for the Degree
Master of Science

Approved July 2015 by the
Graduate Supervisory Committee:

Jitendran Muthuswamy, Chair
Bradley Greger
Jennifer Blain Christen

ARIZONA STATE UNIVERSITY

August 2015

ABSTRACT

Optical Fibers coupled to laser light sources, and Light Emitting Diodes are the two classes of technologies used for optogenetic experiments. Arizona State University's Flexible Display Center fabricates novel flexible Organic Light Emitting Diodes(OLEDs). These OLEDs have the capability of being monolithically fabricated over flexible, transparent plastic substrates and having power efficient ways of addressing high density arrays of LEDs. This thesis critically evaluates the technology by identifying the key advantages, current limitations and experimentally assessing the technology in in-vivo and in-vitro animal models. For in-vivo testing, the emitted light from a flat OLED panel was directly used to stimulate the neo-cortex in the M1 region of transgenic mice expressing ChR2 (B6.Cg-Tg (Thy1-ChR2/EYFP) 9Gfng/J). An alternative stimulation paradigm using a collimating optical system coupled with an optical fiber was used for stimulating neurons in layer 5 of the motor cortex in the same transgenic mice. EMG activity was recorded from the contralateral vastus lateralis muscles. In vitro testing of the OLEDs was done in primary cortical neurons in culture transfected with blue light sensitive ChR2. The neurons were cultured on a microelectrode array for taking neuronal recordings.

TABLE OF CONTENTS

LIST OF TABLES

LIST OF FIGURES

CHAPTER 1

OPTOGENETICS

1.1 Introduction

Proteins perform a vast array of functions within living organisms, including catalyzing metabolic reactions, replicating DNA, responding to stimuli, and transporting molecules from one location to another. The neuron's membrane have naturally occuring protein channels allowing transport of charged ions. These are namely: ion leakage channels, V-gated ion channels, Ligand gated ion channels and the Sodium Potassiom Pump (Samuel, n.d.). Opsins are light-gated proteins which are introduced into the neuronal membrane through chemical, electrical or viral treatment of the neurons.

1.2 Optogenetics

Optogenetics is a neurostimulation technique which combines genetics and optics to control well defined events within the specific cells of living tissue (Deiseroth, 2011). Naturally occurring light sensitive proteins (Opsins) have been extracted from microorganisms like channelrhodopsin reinhardii, bacteriorhodopsin, halorhodopsin. When these light-gated microbial opsin proteins that function as light-activated proteins, are expressed in genetically targeted neurons, the activity of these expressing neurons can be increased or decreased (figure 1) with a millisecond of temporal accuracy (Pashaie, et al., 2014).
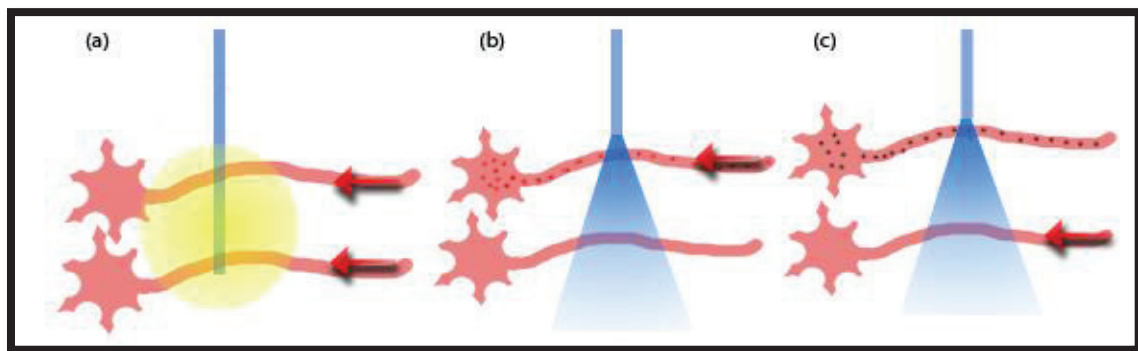
Figure 1.1 a) Electrical stimulus causes nonspecific excitation of neurons b)Depolarizing protein expressing neurons (i.e channelrhodpsin) increases the neuronal activity of such c)Hyperpolarizing protein expressing neurons (i.e halorhodopsin) suppresses the neuronal activity of neurons (i.e influx of chloride ions) (Deiseroth, 2011)

All microbial rhodopsins rely on fundamental photoreaction comprising the isomerization of a covalently bound enzyme which assists the protein (cofactor). The cofactor, when absorbs a photon of light, isomerizes from the so called all-trans to 13-cis structure. This conformal change affects the dipole moment of the molecule leading to structural rearrangements of the protein, which finally leads to the transport of ions. All these rearrangements occur within less than a millisecond whereby the activated opsin goes through various photochemically distinct states (Prigge, et al., 2012). Figure 1.2 shows a four-state electrophysiological photocycle, which explains the major electrical features of channel function, including inactivation, photocurrent kinetics, and adaption phenomena as observed in electrical recordings from cells expressing such opsins[see Figure 1.3]. For example, a fully dark state ChR2 molecule when activated with a short blue light pulse will first proceed through an open state of high conductance (Open State-1, Figure 1.2), causing a peak photocurrent to occur (Figure 1.3) and then translates to a lower conductive state (Open State-2, Figure 1.2) which leads to lower the photocurrent (steady state current, Figure 3). The protein will stay in the conductive states for a duration - Desensitization Time (T_{des}, for ChR2 T_{des} = 10 ms). The molecule will go the dark state in a time $T_{1,2off}$ of 21ms. If the cell is stimulated again at this stage, it will give a photocurrent lesser than the peak photocurrent. For getting current equal to the peak photocurrent, the opsin will have to remain in the dark stage for a duration more than the recovery time ($T_{recovery}$ =6 seconds). (Pashaie, et al., 2014)

A good variety of proteins with varying kinetics(variable T_{on}, T_{des}, $T_{1,2off}$), photocurrent wavelength selectivity, photocurrent magnitudes have been engineered (Mattis, et al., 2012). These variants have been made by point mutations, extraction of opsins from algal species and chimeras constructed by combining opsins. (Mattis, et al., 2012)

Some of the opsins with their kinetic and photocurrent sensitivities are listed in the Table 1 for reference. For the purpose study of Organic Light Emitting Diodes, ChR2 and C1V1tt are of key interest. The OLEDs to be tested have the capacity to activate these two light gated proteins.
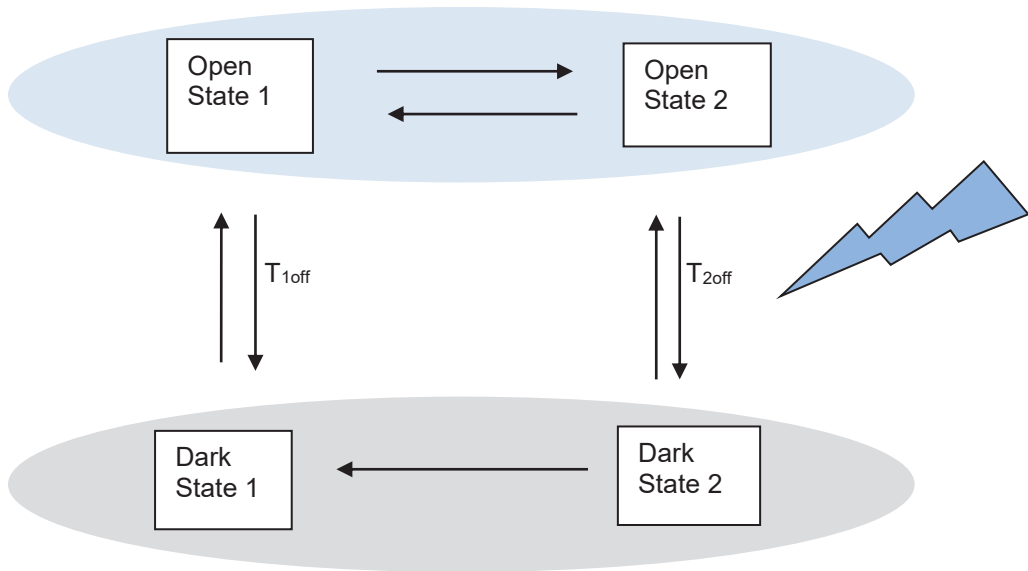
Figure 1.2 State diagram of a light gated protein which can be expressed in specific cell types including neurons (Pashaie, et al., 2014)
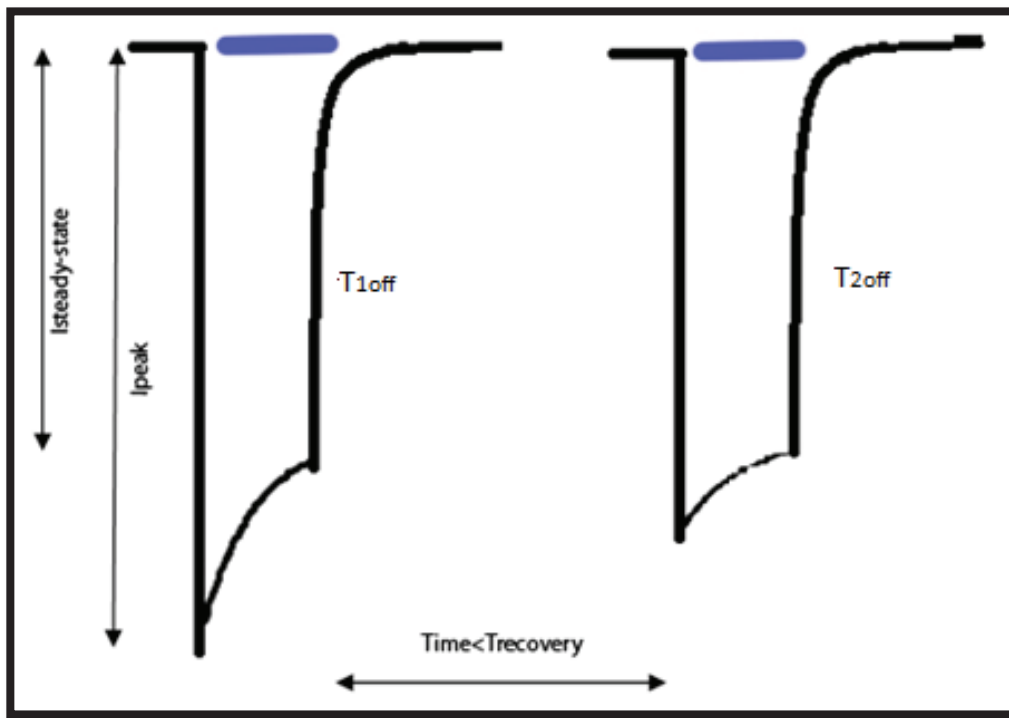
Figure 1.3 Impact on current levels due to interaction of light and light-gated proteins (Opsins) (Pashaie, et al., 2014)

Table 1.1 Hyperpolarizing Opsins and their characteristic properties, extracted from (Mattis, et al., 2012)

Depolarizing agent	Peak Photocurrent wavelength (nm) selectivity	EPD50 peak (mW/mm2)	Time to peak T_{on} (ms)	Time for desensitization T_{des} (ms)	$T_{off(ms)}$
ChR2	**470(blue)**	**1.25**	**9**	**32**	**12**
ChR2$_R$	470	0.7	9	25	25
C1V1	535(green)	0.5	16	56	56
C1V1$_{tt}$	**535**	**0.75**	**17.5**	**75**	**75**

The term EPD50 refers to effective power density for 50% activation. Since the photocurrents are highly dependent on the cell type, promoter, expression level and also the opsin, this parametric tries to provide a parameter independent of these factors. For further statistically unbiased parametric justification of the parameter please see (Mattis, et al., 2012). T_{on} is the time taken to the maxium photocurrent. T_{des} is the time duration for which any other stimuli won't have any impact. T_{off} is the time for the photocurrent to get back to baseline.

Based on the above discussion, a few fundamental principles have been established for activation of excitable cells expressing such proteins. (1) The light intensities should be enough to rapidly open up the channels so that enough photocurrent develops which can bring the neuron past the spiking threshold and then close rapidly to allow the neuron repolarize. If the light is on for more than allotted duration, the photocurrents desensitize, which can lead to spike failures. Hence the duration for which the light is turned on has to be controlled. (2) Also, the more sensitive the protein is the lesser the optical intensity will be required to activate the cells, and more optical intensity will activate higher volume of tissue (Mattis, et al., 2012).

The OLED technology used as a light source in this study has advantages(Discussed in chapter 2) over the iLED technologies for use in Optogenetic experiments. Currently, Blue, Green and Red OLEDs have been fabricated. Based on the intersection of operating conditions of the OLEDs, and kinetic requirement of the Opsins(detailed in the last paragraph), Opsins: ChR2, C1V1tt and Chrimson can be gated with Blue, Green and Chrimson(not discussed) respectively.

CHAPTER 2

ORGANIC LIGHT EMITTING DIODES FOR OPTOGENETIC EXPERIMENTS

2.1 Current Optogenetic Brain Interfacing Technologies And Place Of Oleds

For optically stimulating targeted neurons two classes of light sources: Light Emitting Diodes and Lasers coupled to Optical fibers are used. Both technologies have been utilized for stimulating superficial neocortical and sub regions of the brain, though laser coupled optical fibers are more widely utilized (Aravanis AM, 2007). Laser is highly collimated source of light, which can also be very highly intense. Also the light beam can be very small in several microns range. But since the laser light source is bulky, it limits its use in free behavioral experiments. More recent advances in Light Emitting Diodes have reduced the dimensions($25x25um^2$) of the LEDs while keeping the optical intensities high (McCall, et al., 2013). Such LEDs have been injected and released into deeper structures of the brain (Kim, et al., 2013). For optically stimulating multiple sub regions of the brain SU8 based waveguides sourced by mounted micro-LEDs have been shown to work. Utah Optrode Array is a glass or a silicon structure currently sourced by Optical Fibers coupled to lasers, is structurally equivalent to the Utah Electrode Array (Abaya, Blair, Tathireddy, Rieth, & Solzbacher, 2012). Other efforts in spatially addressing sub regions of the brain include: micro machined optical fibers (Pisanello, et al., 2014), Devices using LED or Laser light source coupled waveguides each exciting a specific sub region of the brain have been developed. Some such examples are glass-sharpened optrodes (Royer, et al., 2010), arrayed optical fibers, endoscopic fiber bundles, and wireless micrometer-sized LEDs on flexible shafts. Recently, for generating 3D distributed light patterns in the brain, Individual waveguides can be addressed by a matrix of micromirrors separately coupled to different light sources, allowing optical stimulation at each point with tunable wavelength and intensity (Anthony N. Zorzos, 2012).

In all the above described neurotechnologies the standard fabrication techniques for fabricating them are electrospinning, chemical vapor deposition, thin film spin casting and lithography (Anikeeva, 2013). The light source attachment is a mechanical semi-automated process. No currently existing technique allows integration of the light source onto the substrate as an integral step of the fabrication procedure. As a result Light sources can be integrated with

the electrode arrays for neural recordings as well as the electronic components supporting them -

all on the same substrate.

Organic Light Emitting Diodes have features which can aid in development of scalable,

high throughput, flexible, arrayed, efficient active matrix addressed optical stimulation recording

electrodes. OLEDs used in this report have been fabricated using standard semiconductor

fabrication techniques at lower temperature.

2.2 Organic Light Emitting Diodes

Conventional Thin Film Transistor (TFT)-based OLED displays are produced on rigid and

fragile glass substrates (fig 1a). For the purpose of optogenetic experiments, this fragile substrate

has been replaced with a flexible 125µm thick flexible Dupont Teijin Films Teonex® polyethylene

naphthalate (PEN) transparent plastic substrate (Figure 2.1b).
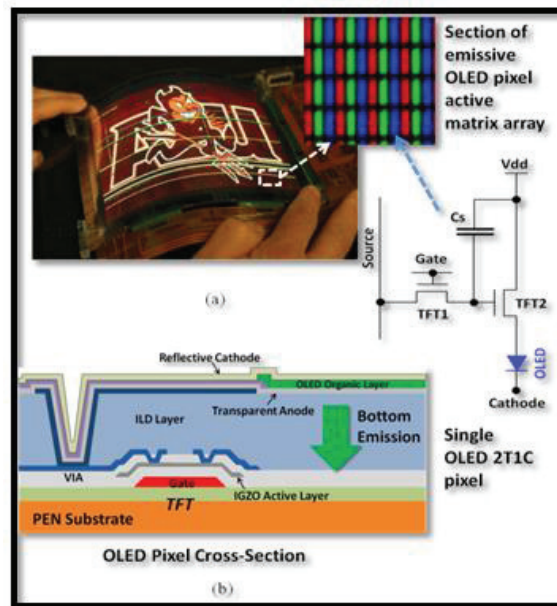
Figure 2.1 (a) Photograph of flexible color OLED display on PEN plastic substrate, with a small region of the display magnified to highlight the individual three color OLED pixels along with the circuit schematic for the two transistor, 1 capacitor b) cross-section of the flexible OLED (Smith, O'Brien, Lee, & Bawolek, 2014)

An active matrix LED array differs from a discrete LED array. In active matrix LED there

is an addition of two TFTs and one capacitor (2T1C) per LED element, while each element in a

discrete array uses one LED plus interconnect wiring. The key difference between active matrix LED and OLED array is that, in case of OLEDs the 3 elements: 2T1C are integrated on the same substrate and formed using micron and sub-micron scale-patterning TFT manufacturing process sequence (fig1a, b). In operation, the thin OLED organic layer shown in fig 2b emits a bright light when a forward voltage bias is applied across the transparent anode and reflective cathode terminals (Smith, O'Brien, Lee, & Bawolek, 2014).

Bottom-emitting blue OLED structure is shown in the Figure 2.1a. These were fabricated on flexible PEN plastic substrates at the Arizona State University (ASU) Flexible Display Center (FDC). The detailed fluorescent blue OLED device structure consists of injection, transport, and blocking layers, along with the emission layer. These are abbreviated in Figure 2.3b as HIL (hole injection layer), HTL (hole transport layer), HBL (hole blocking layer), ETL (electron transport layer), and EIL (electron injection layer). A reflective aluminum layer is used to form the cathode, and the anode is a transparent indium tin oxide (ITO) layer located directly under the HIL. The emissive layer used for this effort is a single host doped with a blue fluorophore, where the injected electrons and holes recombine to emit a (bright) blue 455nm light (figure 2.2a). The fabrication procedure and optical characterization is detailed in (Marrs, Moyer, Bawolek, & Cordova, 2011), (Gregory B. Raupp*, 2012), (Smith et. al. 2014).

2.3 OLED CHARACTERISTICS

When the OLED is operated in the pulsed mode rather than in static mode, it can tolerate higher voltages and consequently emit higher power densities as shown in the figure 2.3 a,b. From the discussion in the Chapter 1 on the kinetics of opsins, operating the blue or the green OLED at 10Hz frequency is a suitable for depolarizing the ChR2 or C1V1 expressing neurons respectively.
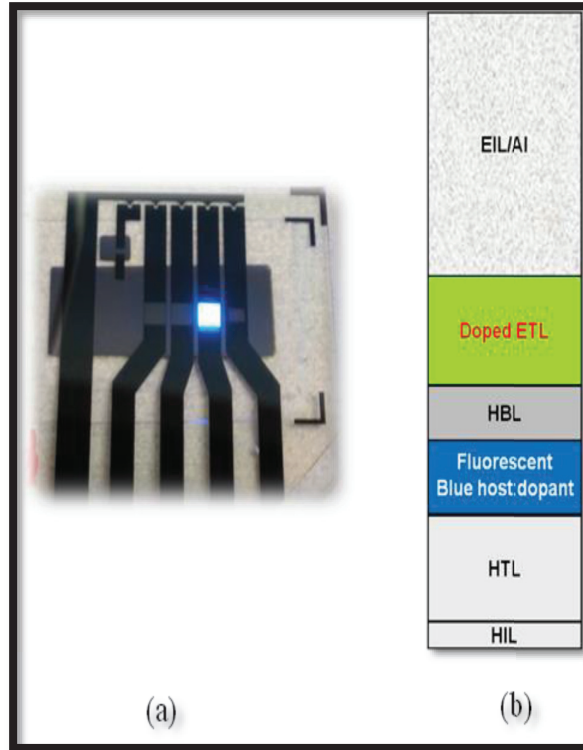
Figure 2.2. (a) A blue OLED structure (b) Detailed structure of the fluorescent Blue OLED structure (Smith, O'Brien, Lee, & Bawolek, 2014) HIL (hole injection layer), HTL (hole transport layer), HBL (hole blocking layer), ETL (electron transport layer), and EIL (electron injection layer)
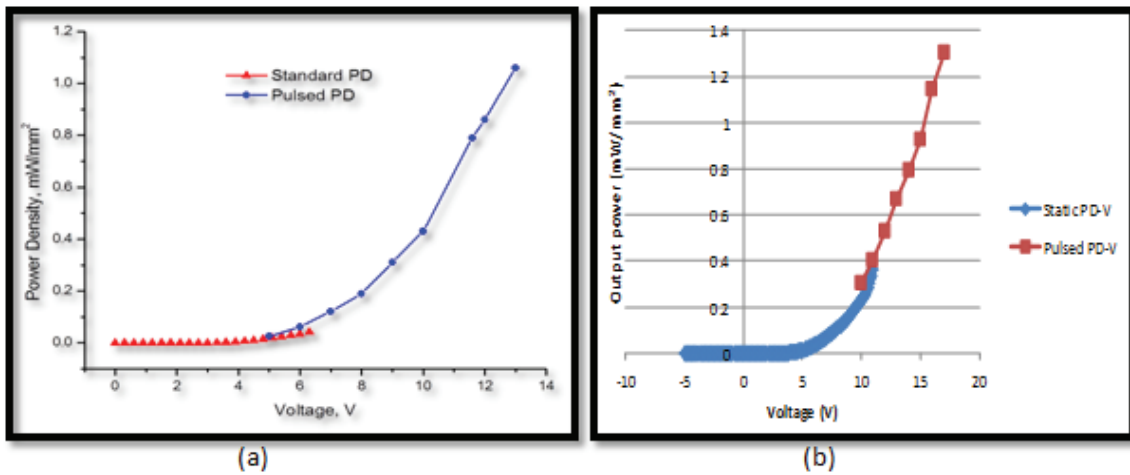
Figure 2.3 a) Blue OLED Power Density curve b) Green OLED Power Density curve; in the static mode voltages have been incremented from 0 to 6.5 V in fig2.3a and from 0 to 11V in fig1b with 0.1V increments, and in pulsed mode with 10msec pulse width and 10Hz period voltages have been varied from 5 to 13V in fig 2.3a and 10-18V in 2.3b (Smith, O'Brien, Lee, & Bawolek, 2014)

For the purpose of comparison of the OLEDs with respect to the commercially-available LEDs

(Nichia NSPB300B, which have been already shown to work for optogenetic experiments (Iwai Y,

8

2011)). OLEDs and iLEDs (commercial LED is made out of inorganic material) were compared on Photoluminiscence(PL) setup in the Optocharacterization lab of Dr. Yong-Hang Zhang at Arizona State University.

The setup consists of a series of lenses to collimate the source of light into a spot and direct it to an optoelectrotronic system to diffract the light based on wavelengths and source them into a photomultiplier tube to make a calibrated reading of the intensity of light.

The operating condition of the iLEDs and OLEDs was 10Hz at 10% duty cycle (same as the operating conditions during optogenetic experiments). It was observed that the spectra of the blue OLED was broader than the spectra of the iLED. The blue OLED is whiter in comparison to the blue iLED(Figure 2.4).

Also, the relative intensity observed in the pulsed mode for the OLED was ~0.1% of the iLED(Figure 2.5). This low relative intensity could be attributed to several reasons including - low shelf life of the OLEDs (hence intensity degrades over time), or lower currents being sourced to the OLED.
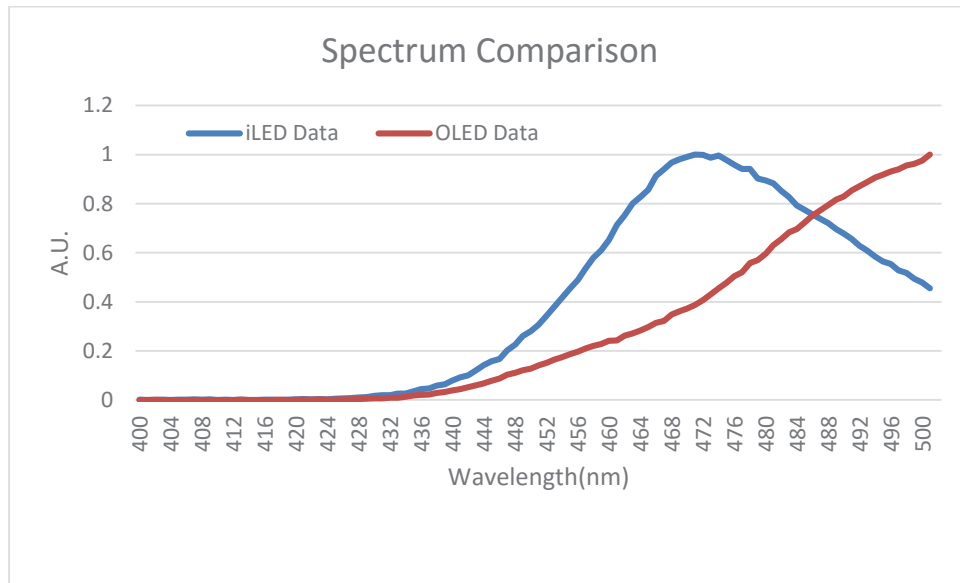
Figure 2.4 Spectrum of OLED vs iLED between 400nm and 500nm
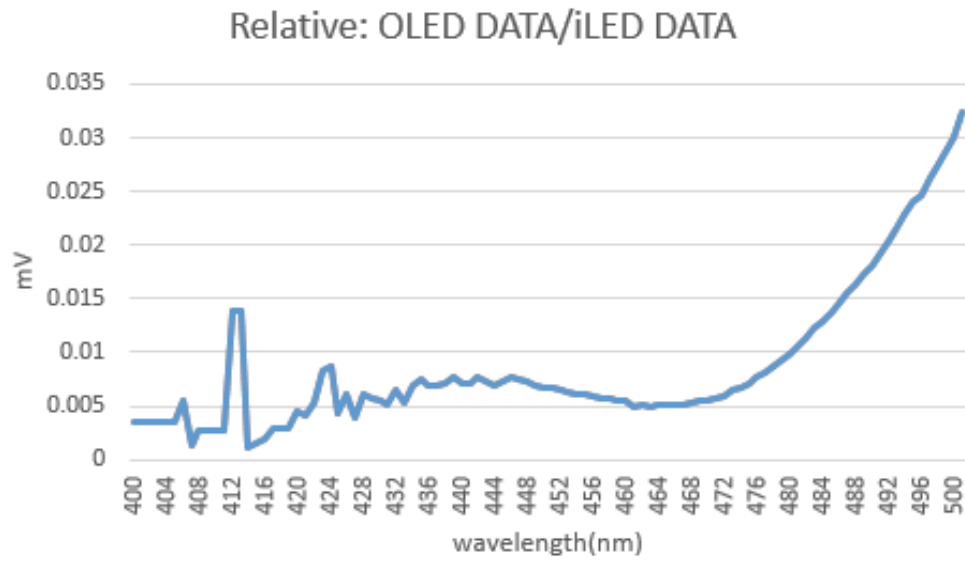
Figure 2.5 Relative intensity of the OLED w.r.t. ILED

CHAPTER 3

INVITRO EXPERIMENTS

3.1 Introduction

The first test of the OLEDS was on the in vivo animal model. Primary cortical neurons were stimulated using the OLEDs and neuronal activity was recorded(Figure 3.1). A change in the firing rate recording to light response was estimated. For this primary cortical neurons are cultured over dishes with indium tin oxide based microelectrodes arrays(MEAs)with 32 recording channels(Figure 3.2b). ITO based microelectrode arrays were fabricated in the clean room using previously established methodology. Briefly the method involved deposition, pattering of photoresist and etching to sequentially fabricate chrome bond pads, microelectrodes, traces and Parylene-C insulation over the ITO substrate (Patel and J., 2012). The final product has a transparent outlook with 32 microelectrodes insulated with Parylene-C. The MEA was connected to Plexon amplifier using a custom printed circuit board(PCB)(Figure 3.2e).

The neurons thus seeded are then chemically transfected with either with ChR2 or C1V1tt plasmids at 2-3 DIV/7-8 DIV respectively. Neural recordings are taken on the day after transfection.
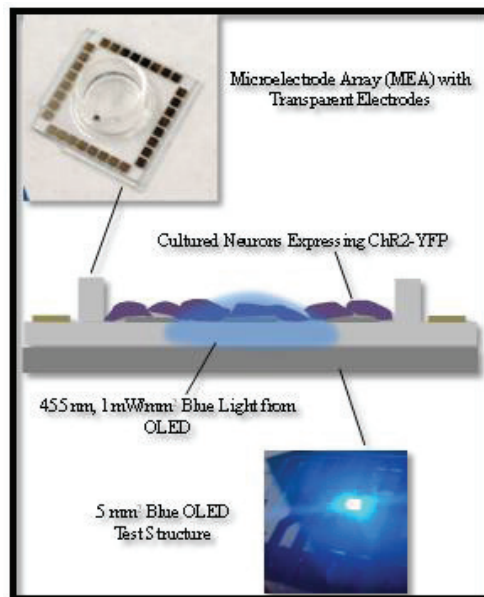
Figure 3.1 Blue OLED invitro experimental setup [Illustration Courtesy: Dr.Jennifer Blain Christen]

3.2 Methods

The various steps in culturing, transfection and recording of the neurons are described below. All the equipment in the culture has to be sterile and autoclaved. Before and after every use of the Biosafety Cabinet is cleaned with 70% alcohol and kept in UV for 20 minutes.

Primary Neuron Culture Protocol

Microsurgically dissected cortex tissue from E18 Sprague Dawley Rats were purchased from BrainBits LLC. Neurons arriving thus are seeded on sterile autoclaved MEAs as soon as possible to increase the yield of the neurons. These can however be stored at 4-8℃ for one week. NbActiv1 ™ for cortical tissue is used as a media for the neurons.

Microelectrode Array Preparation

Microelectrode array surface needs to be prepared for neuron seeding. Obtain Polyethyleneimine dilute it to 1:1000 in DI water. Place 300 uL on each MEA. Let it sit overnight, or atleast 1 hour. Remove and rinse the MEA's with sterilized distilled water. MEAs are only then ready to be placed with neurons

Neuron Preparation

Take out 1 mL of media without taking out the neurons and put it into the 15 ml tube. Mechanically triturate the tissue up with a 1 mL pipette and place into 15 ml tube. No more than 30 times maximum (ideally 10-15). No tissue should be visible afterwards.

Remove media from the side opposite of the neurons. Calculate the number of cells using a hemocytometer. Depending on the concentration required, put 1 mL or more of new media into it. Slowly resuspend the neurons using the pipette. Put in the center of each MEA, 25 µL of neurons. Let incubate for 1 hour and then add 300 µL of media

Transfection

As noted in the discussion in the previous chapter, ChR2 is a blue light sensitive depolarizing construct. Fubi-ChR2-GFP(addgene plasmid #22051 (. Boyden ES, 2005)) with a 5' target sequence GCACCTTTTGAAATGTAATC 3' were transfected on cortical neurons seeded at ~3000 cells/mm² 3 DIV. Fubi-ChR2 was complexed with pre-formed polyethyleneimine (Aldrich, CAS#9002-98-6) with a 1mg/ml stock -solution in distilled water. Next 1μL of Fubi-ChR2 and 1μL of PEI stock solution in 8μL of distilled water was incubated for 15 min to form the delivery complex. Cells in NbActiv1™ medium (Brainbits, LLC, Springfield, IL) were incubated with Fubi-ChR2 for another 15 min, after which the solution was removed and replaced with fresh media. Live assay was performed using Calcein AM (Anaspec, Fremont, CA) assessed cell viability at 1 hour after transfection using florescence microscopy (Leica).

Combine Lipofectamine(Lipofectomine LTX Reagent, invitrogen) and Media in a proportion of 2:98. For ChR2: Combine 100uL of the Lipofectomine solution to a solution of 90 uL media and 10 uL genetic material; Make sure to remove media on neurons then add 200 uL of media. Incubate for 4-5 hours. Remove all media and add 300 uL of fresh media (change every third days) . All the Neuron Media, NbActiv™ used in this study had been filtered using 25um pore size filters.

Live Dead Assay

This technique is used to visually estimate the live neurons/cells. For this, the neurons are washed 3 times using PBS solution . A 1:1000 dilution of the Biotium(Viability/Cytotoxicity Kit for Animal Live & Dead Cells) with a volume of 10uL is kept standing for 20 minutes on the washed neurons. Using a fluorescence microscope with a GFP filter, the live neurons can be easily distinguished.

The actual setup for in vitro optogenetic experimentation is shown in the figure 3.2. A Plexon amplifier was used in all the in-vitro experiments. The entire apparatus(Figure 3.2E) was kept in a faraday cage to get low baseline noise of $\sim 5 - 8uV$.
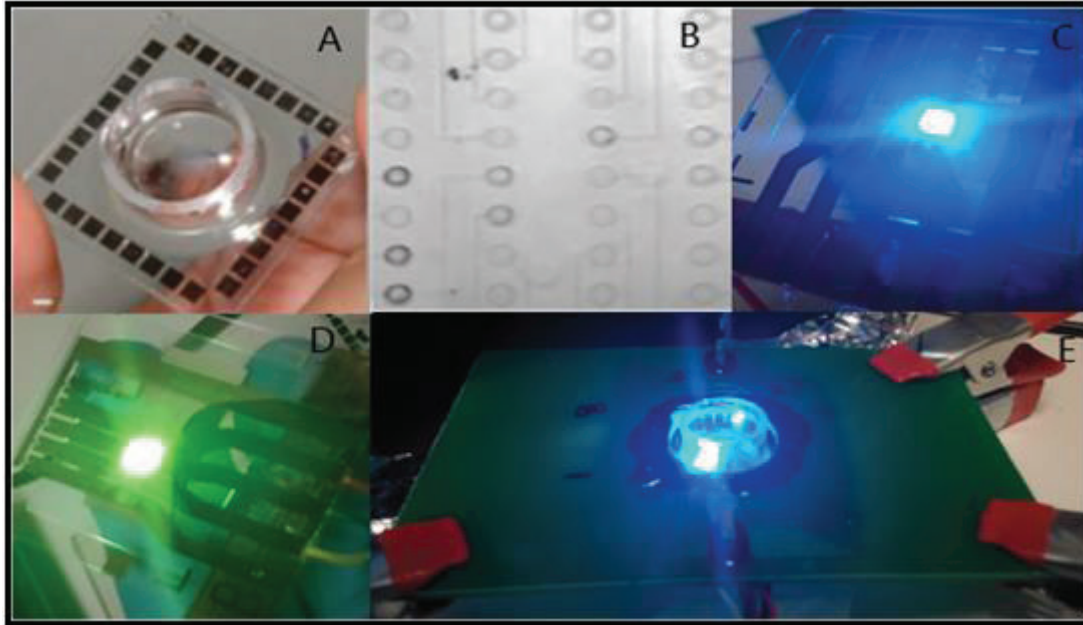
Figure 3.2 a) The culture vessel b) Patterned Mircoelectrode array on the vessel c) Blue OLED d) Green OLED e) The invitro optogenetic setup for neurons transfected with ChR2

3.3 RESULTS:

In one round of experiments ChR2 tagged with green flourescent protein (GFP) were used and in another round of experimentation ChR2 tagged with yellow flourescent protein was used.

For the first set of experiments, the neurons were transfected with ChR2 tagged with YFP 5 DIV. 16 channels had been recorded at a time. Each MEA has 32 electrodes to record from. The OLED was turned on for a duration of ~2 seconds. The OLED was operated in the pulsed mode with Peak to Peak voltage 14V and at 10Hz, 10% Duty Cycle. The 2 second pulse train was followed by 10-12 seconds of silence(the recovery time of the Opsins ~6 seconds).

The detailed analysis of the neural recordings was done on Plexon Offline Sorter(Figure 3.3) and MATLAB(Figure 3.4,3.5). The distinct wave shapes were identified in the PCA space. Wave shapes characteristic of the photo-electrochemical effect and non-characteristic neural wave shapes were removed from the analysis.

Data in the Figures 3.4 are for the transfected channels with varying levels of expression of the Opsins. For channel 3 the firing rate during stimulation with respect to before and after stimulation is different with a confidence interval of 90%, likewise in channel 15 it is different with

a confidence interval of 99.999% Figure 3.5 show the channels 1 and 7 which did not show a significant increase in the neural activity post optical stimulation.
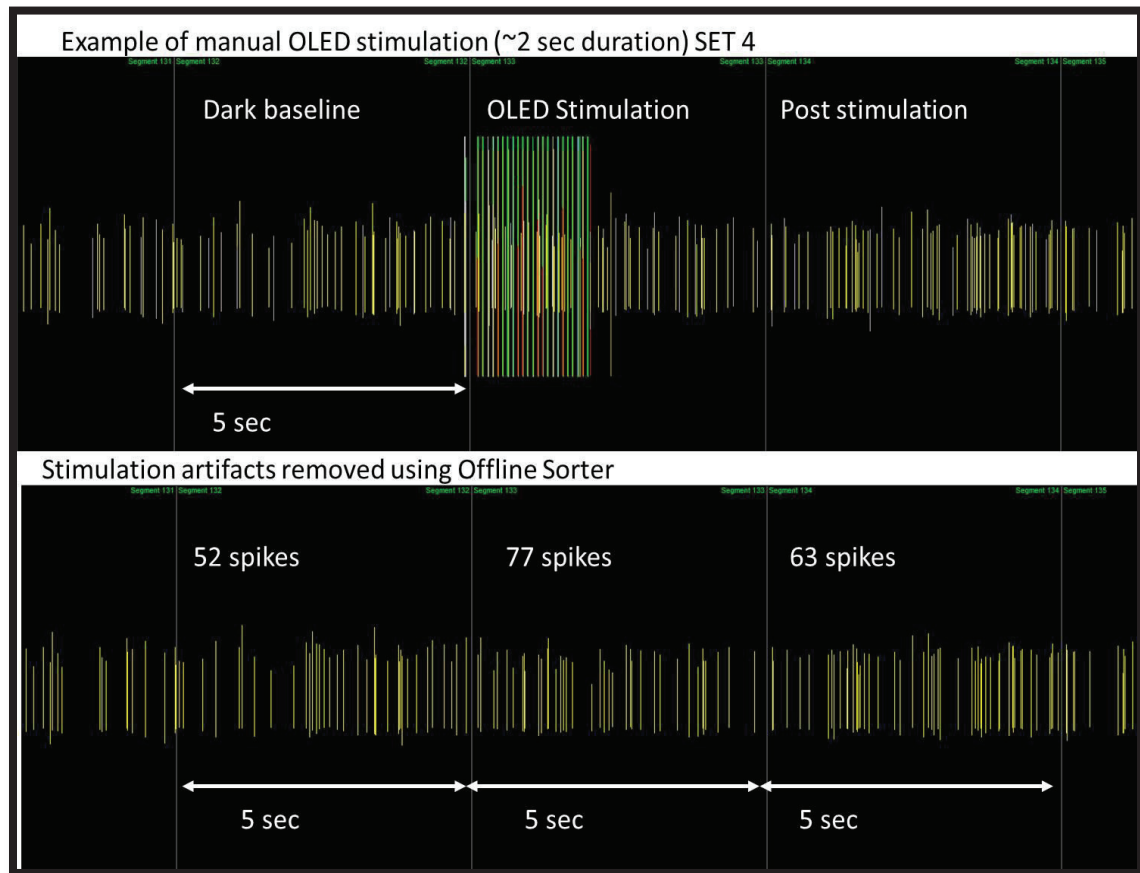
Figure 3.3 Raw spikes detected on Plexon offline sorter(top), The stimulus artifact has detected and removed from via the PCA space

The pre and post stimulus neural activity wave shapes are aggregated and shown in the Figure 3.6. All the wave shapes are characteristic of neural signals which was the basis for considering or rejecting sorted wave shapes. Blue and Red waveforms and pre and during stimulus waveforms respectively. Black and Green are respectively the average waveforms of pre and during optical stimulus.
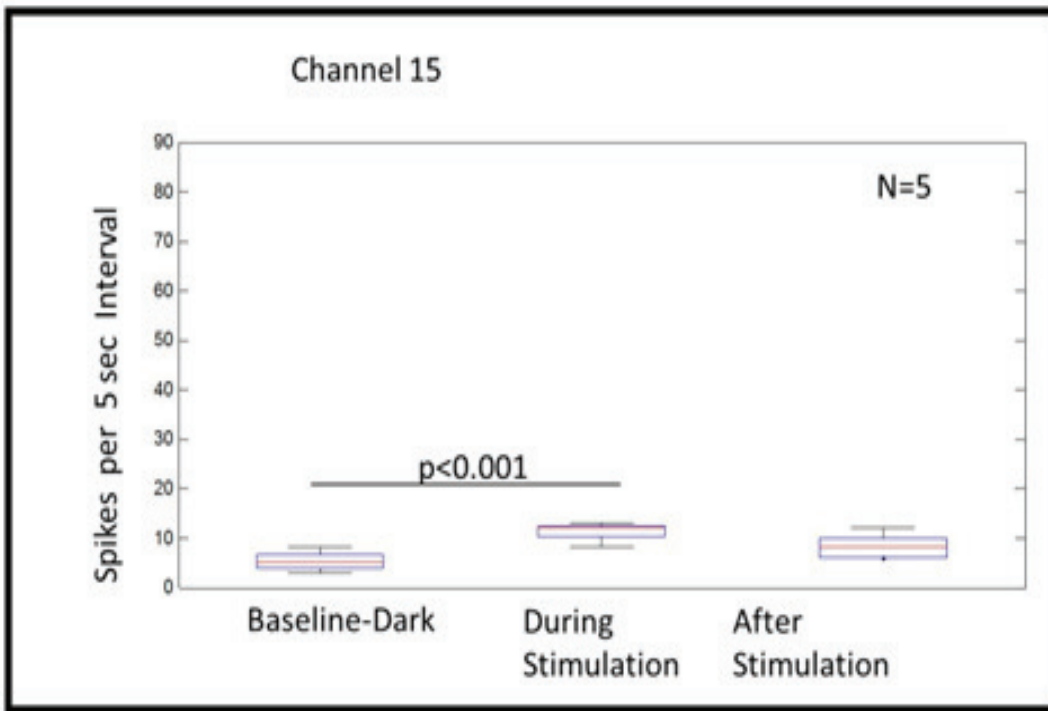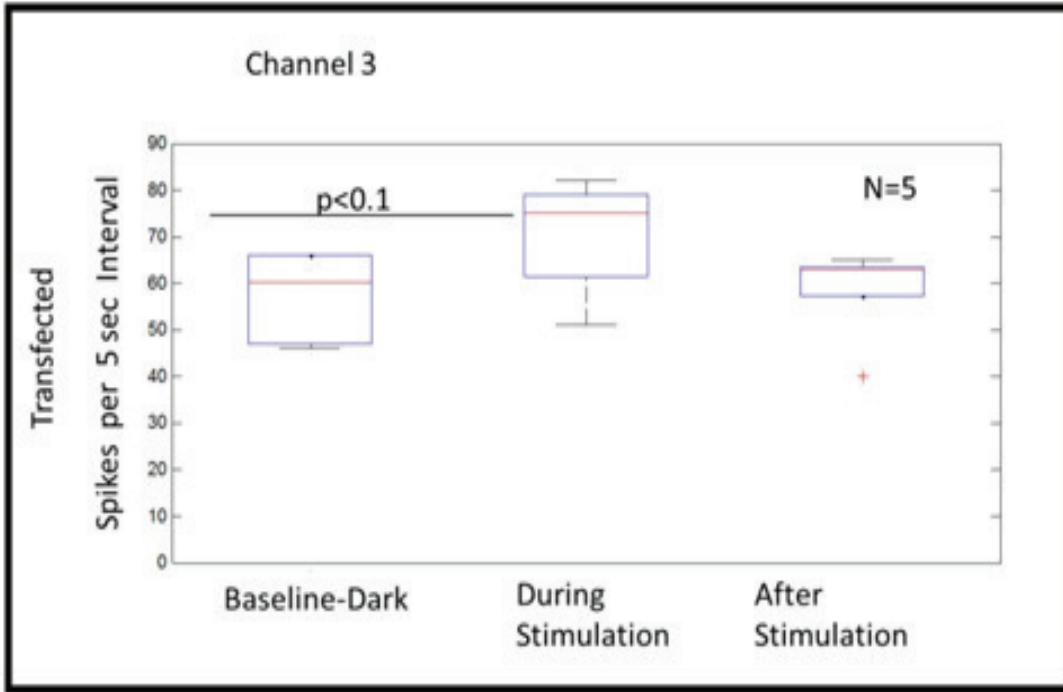
Figure 3.4 Statistical analysis performed on Matlab on the sorted Plexon data to create the Box Plot(student's t-test), and determine channels showing significantly higher neural response to optical stimuli
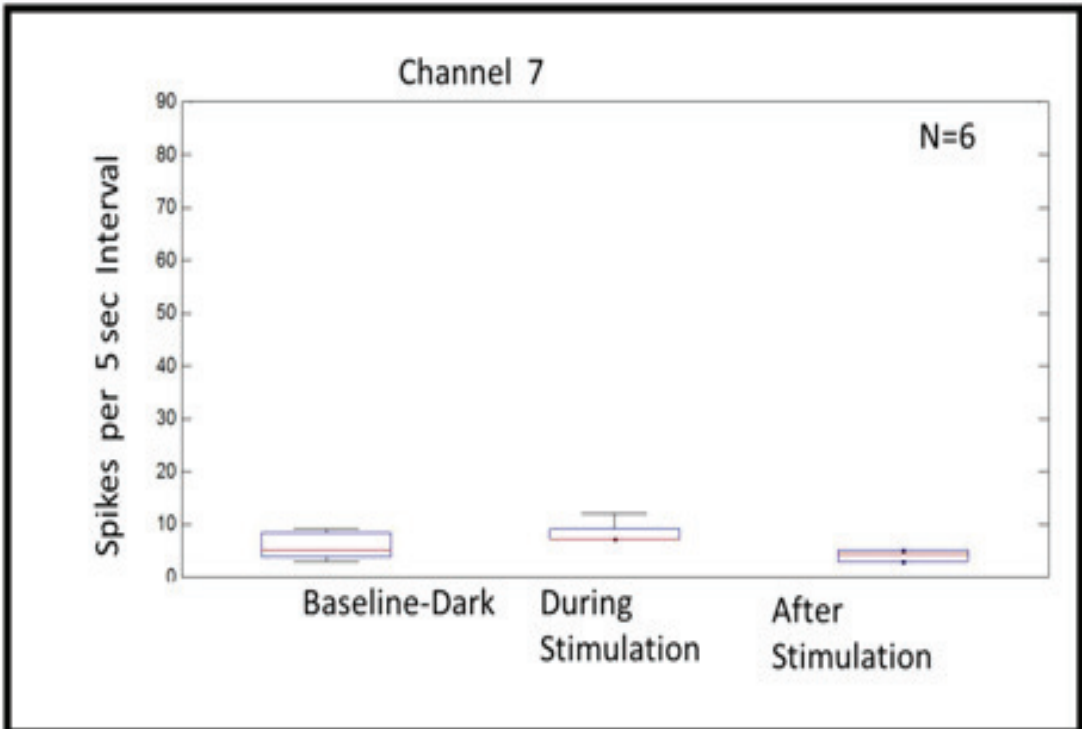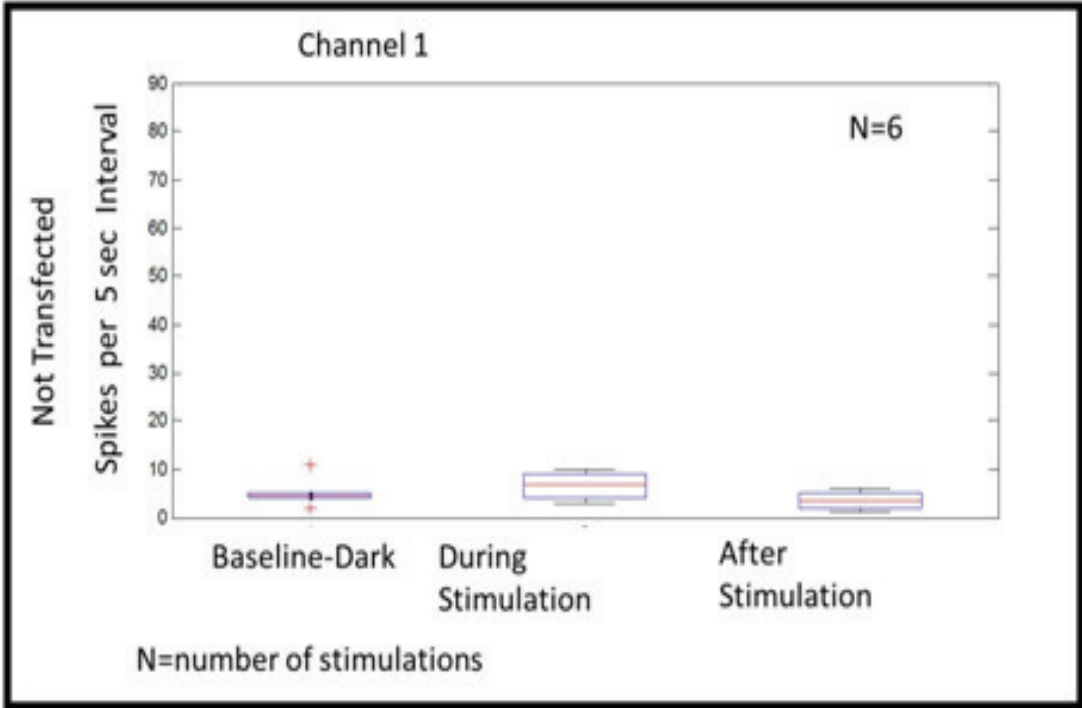
Figure 3.5 These are 2 channels which do not show response to optical stimulus, and hence are expected not to be transfected.
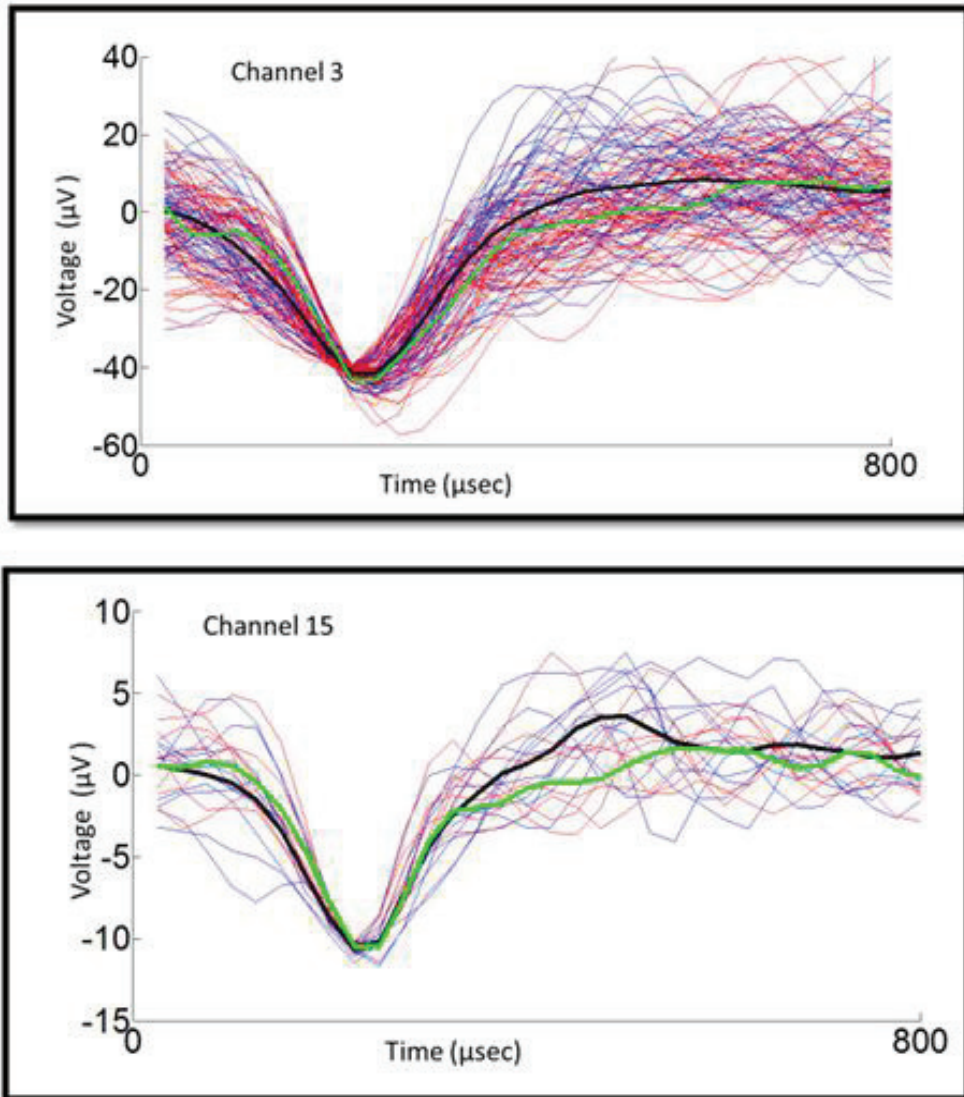
Blue = raw waveforms before stimulation over 5 sec interval
Red = raw waveforms after stimulation over 5 sec interval
Black = average waveform from before stimulation
Green =average waveform from after stimulation

Figure 3.6 Time aligned waveforms of the channels showing significantly higher neural response upon optical stimulus

After the above set of experiments, a live dead assay test was done on the neurons to check the viabilty of the neurons(Figure 3.7). This shows that a large majority of the neurons are alive.
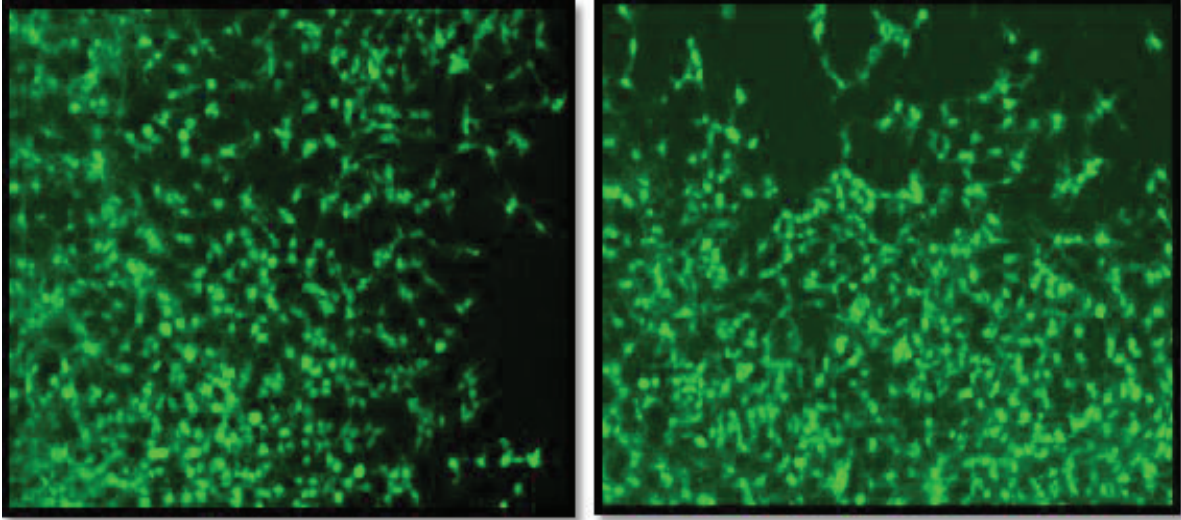
Figure 3.7 Live Dead Assay performed on the Vessels with neurons showing Optogenetic activity using blue OLEDs

In a later experiment, ChR2-GFP was transfected 5 DIV using a similar procedure to that described earlier. Successful transfection of 10% of live neurons was achieved. Out of 16 channels recorded, 4 channels showed optical stimulus response.

For the second round of experiments, the neurons were transfected with ChR2 tagged with GFP 5 DIV.
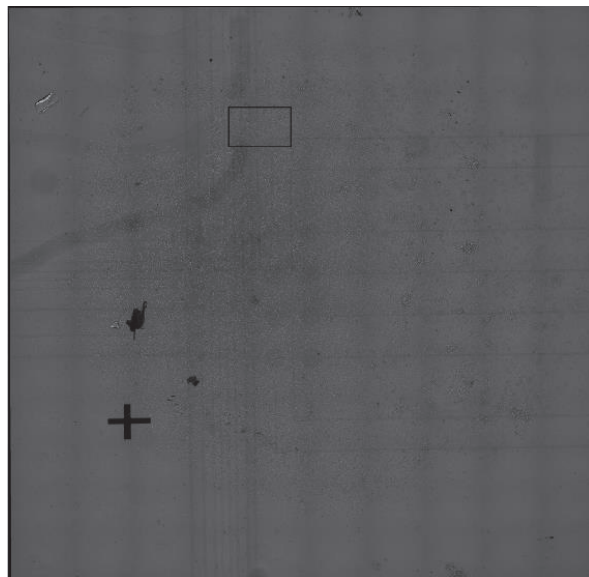
Figure 3.8 The entire MEA seeded with neurons, second round of experiment (Boxed region is zoomed into in the next figure)
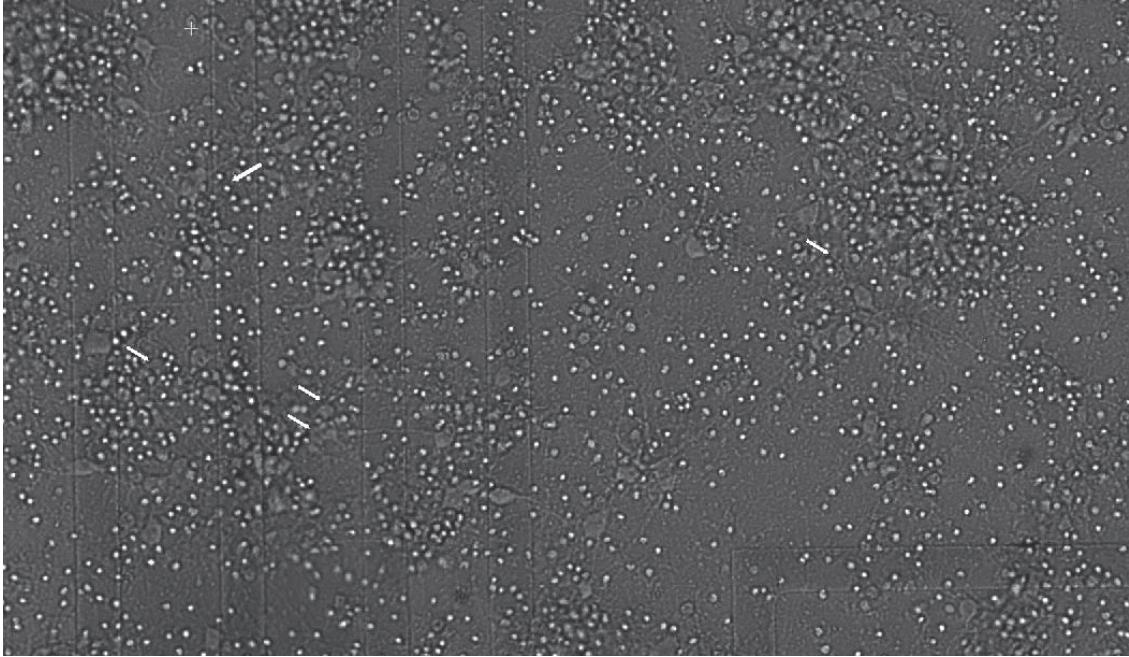
Figure 3.9 Neurons overlaying the traces of the MEA(Boxed region in the previous figure)
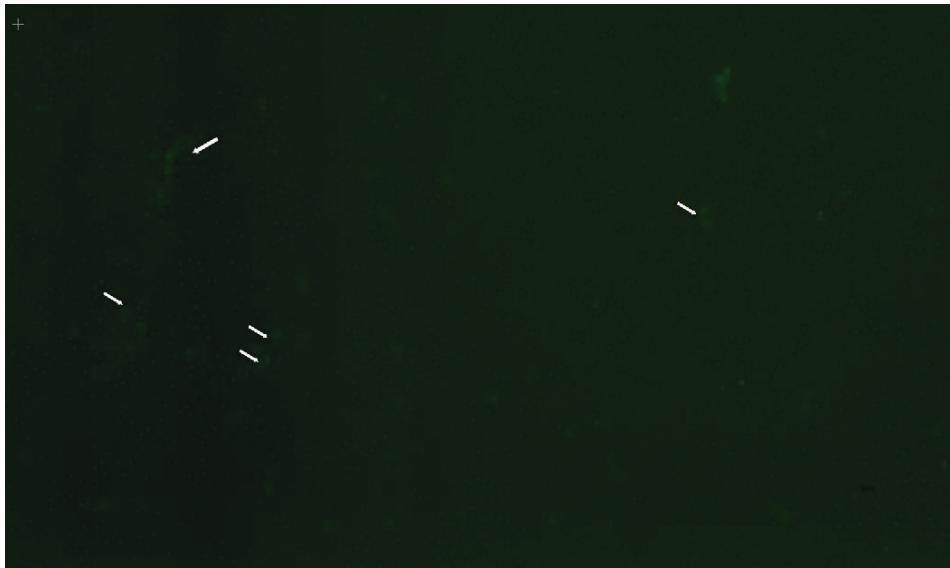
Figure 3.10 Successfully transfected neurons overlaying the traces of the MEAS

16 channels had been recorded at a time. Each MEA has 32 electrodes to record from. The OLED was turned on for a duration of ~7 seconds. The OLED was operated in the pulsed mode with Peak to Peak voltage 15V and at 10Hz, 10% Duty Cycle. The 7 second pulse train was followed by 7-8 seconds of silence(the recovery time of the Opsins ~6 seconds). Figure 3.8 shows the entire MEA(stitched image, Leica) which has been seeded with neurons. The square

box has been zoomed into in the Figure 3.9. This is the bright field image(Leica). In the Figure

3.10 fluorescence microscopy shows the neurons which have been transfected. The arrows in

Figure 3.9 and 3.10 correspond to the respective neurons which have successfully transfected.
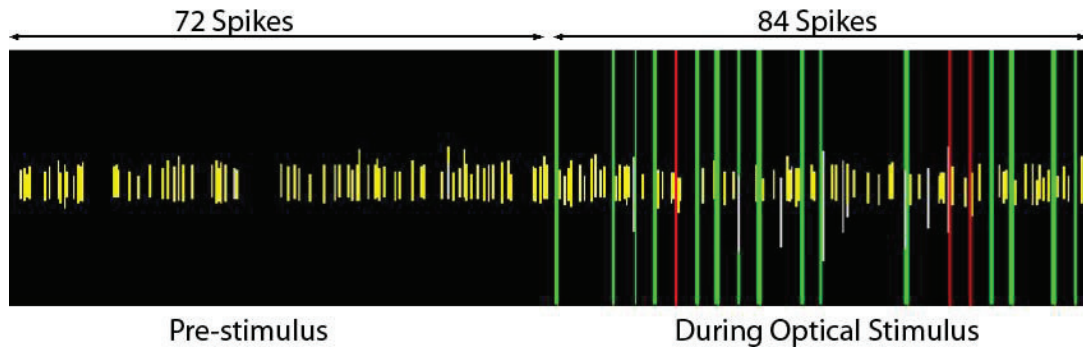
Figure 3.11 Channel 4 Pre-stimulus activity
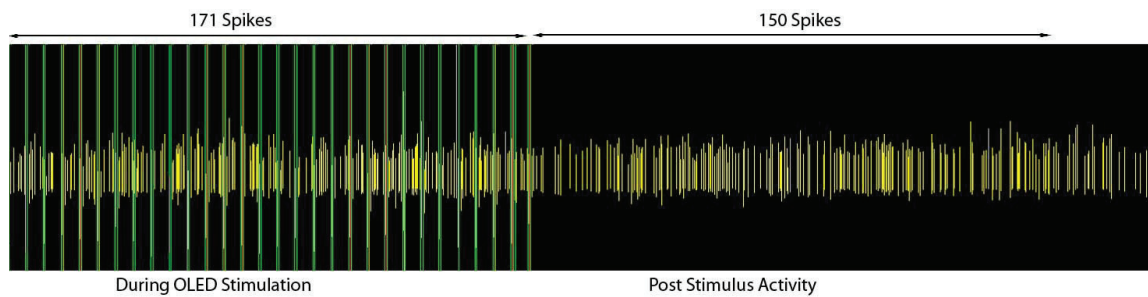
Figure 3.12 Channel 12 Post stimulus activity

Figure 3.11 and 3.12 show the pre/during and during/post stimulus activity in channels 4

and 12 respectively. Likewise, Figure 3.13a,b shows the pre/during and during/post neural activity

of the channel 9.
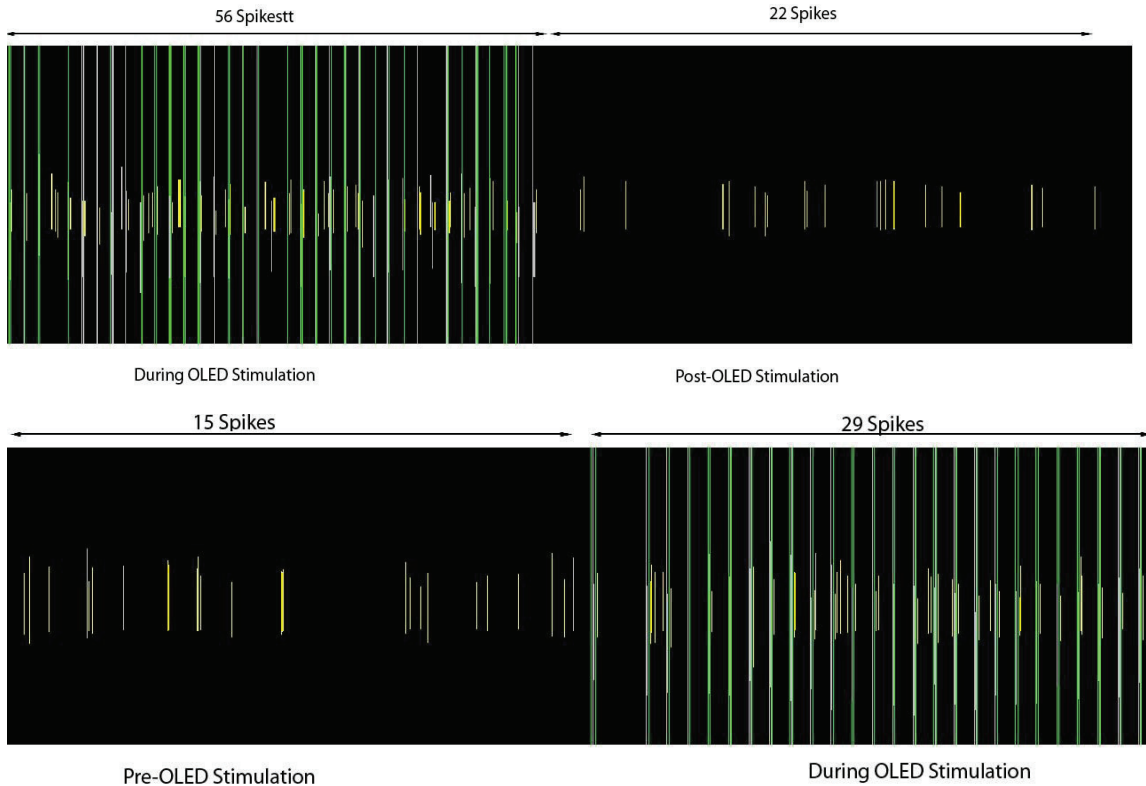
Figure 3.13 Channel 9 a) Post Stimulus Activity b) Prestimulus Activity

3.4 Discussion

Based on the above results it is convincingly shown that the blue OLEDs can in fact stimulate neurons in-vitro. The neural recordings are averaged over a 5 second duration in the above discussion. Since the dimensions of the Microelectrode is at least 10x the average diameter of the neurons, the recordings are expected multi-unit recordings rather than single unit. If precise patch clamp recording are taken, the ChR2 expressing cells will time synchronously depolarize in response to optical stimulus. On the other hand, in our analysis we have eliminated the duration of the optical stimulus, because of the capactively coupled artifact. This is one of the disadvantages of the LEDs. Since the leads for LED are open, the voltage gets coupled between the electrodes and the leads which is in turn amplified by the neural amplifier. Since the density of neurons is high, the activation of some ChR2 expressing neurons is going to in turn activate and depolarize the network of neurons surrounding it. Hence, even between the 2 pulses (90

22

milliseconds apart), when the light is off, the neurons are expected to fire at a higher rate than the baseline activity. This was understandably the case in our experiments.

It is also worth realizing that not many channels showed increase in neuronal activity in response to optical stimulus. This is very likely because of the chemical method of transfection employed which usually has a low transfection efficiency in the range of ~5%(first experiment), ~10%(second experiment).

CHAPTER 4

IN VIVO EXPERIMENTS

4.1 Introduction

To test the organic light emitting diodes in vivo the experimental design consisted of the following experiments performed on both control non-transgenic mouse models(C57BL/6J, from Jackson Labs) as well as transgenic mice(B6.Cg-Tg(Thy1-COP4/EYFP)9Gfng/J, from Jackson Labs).

The following experiments were performed on each animal:

1. Intra Cortical Microsctimulation of the motor cortex(stimulating M1 motor cortex - activating the contralateral hind limb and front limb)

2. Commercial LED - direct stimulation(same location as ICMS)

3. Organic Light Emitting Diodes - direct stimulation(same location as ICMS)

4. Organic and Commercial LEDs tested out using a custom built light collimating system. (same location as ICMS)

What follows is a detailed discussion on the craniotomy procedure, ICMS electrode design EMG electrode, Collimating System Design, Optrode Design and the experimental results.

4.2 Methods:

Rat, Mouse Handling And Craniotomy:
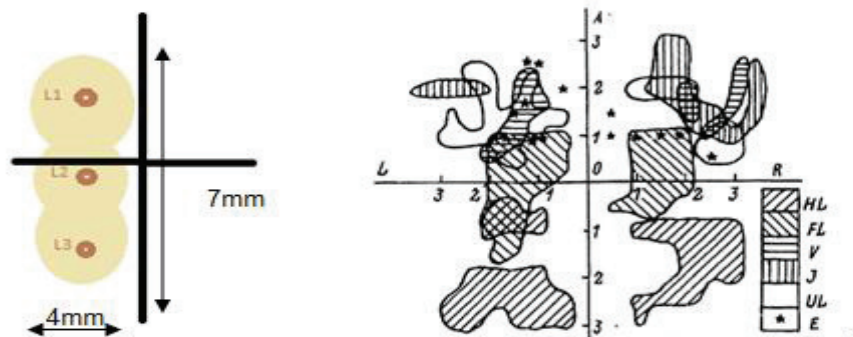
Figure 4.1 Left: Location of the craniotomy in mouse, Right: Motor Map for mouse (Young, Vuong, Flynn, & Teskey, 2011), (Pronichev & Lenkov, 1998)

24

The ICMS experiement was first tested out on the rat animal model. Ketamine xylazine acepromazine was given via intraperitoneal (IP) injection to first anesthetize the rat. Soon after the hair on the skull and on the contralateral hindlimb to the craniotomy location was removed. The animal was fixated on a stereotaxic frame with the help of earbars. After cleaning the skin with an alcohol swab or Povidone Iodine, the skin was cut using surgical scissors. The underlying connective tissue was moved towards the sides using cotton tips. The skull was dried using hydrogen peroxide solution. Finally a burr drill was used to make a big craniotomy 3mm anterior and 4 mm posterior to the bregma, and 4 mm lateral to the bregma. An Amscope microscope was used to monitor the drilling to be just enough to make a boundary of the dimension of the craniotomy. The drilling has to be enough so that the region of the skull to be removed, moves slightly upon pressure on the central region perhaps using a tip. At this stage it shall be safe to pick the skull, so that blood vessels are intact clearly visible.

Next the dura has to be removed. If the electrode dimensions 100um or less, the dura won't need to be removed. In our case the electrodes as well as the optrode have a dimension which is higher than that. If the dura is not nicked and peeled, the pressing of the electrode will dimple the dura and compromise the accurate positioning of the microwire at the appropriate depth. The dimpling at one location can also cause eventual damaging of the blood vessels in the surrounding region. If there is bleeding/damaging of the blood vessels it will cause the neurons in the region to silence.

The same procedure is followed for the mouse craniotomy, except for that, instead of KX(as in the rat experiments), isoflourane was used for keeping the mouse on anesthesia. This was given after the initially giving KXA and removing the hair overhead and on the hindlimb. Extra care has to be taken in comparison to the rat craniotomy while drilling not to damage the dura any bit.

Since the mouse craniotomy deserves a lot more careful surgical procedure, a table below lists the various situations that can come up during the surgery.

Table 4.1 Troubleshooting for keeping the subdural surface of the brain intact (Roome CJ, 2014)

PROBLEM	POSSIBLE REASON	SOLUTION
Bleeding from the muscles exposed around the skull region	Too much skin is removed, and roughly handled causing tearing of muscles	Gently pull the skin to cover the muscle and stick the skin using vetbond
Bleeding through the skull	Blood vessel in the skull is disrupted, especially when drilling across the skull sutures	Soak up bload with gelfoam and allow blood to clot before applying agarose
Drill pierces through skill and dura	Excessive pressure or speed is applied during drilling	Discard the animal
Brain swelling and bulging through the craniotomy	Edema caused by heating of the drilling area due to too slow drilling	Reduce the time taken to drill, keep the area cool by wetting it wetting it saline
After removing the cranial bone, the brain surface appears bruised	Subdural bleeding due to blood vessel damage	Discard the animal as the dura has been compromised

For the mouse experiment, the initial KXA dose was used in a proportion, and given at a scale of 0.1ml/25gm animal weight. The succeeding initial isoflourane dose after the hair removal was kept at ~1 lpm, during the latter part of the experiment it was kept at ~0.8lpm. The simultaneous oxygen supply was kept at ~1 lpm.

At times, when the SpO_2 levels fell below 85%, the animal is adjusted to make sure that it can -breathe properly, without its head tilting too high and body positioned close to the earbars. Simultaneously, increase in the oxygen supply to 2-3 lpm has also be experimented and helps to bring the SpO_2 back to normal range (>=92%).

Superficial Optical Stimulation Light Sources

The two light sources used are shown in their on state below, were placed directly over the exposed, motor cortex region while EMG electrodes were implanted in the contralateral hind limbs.
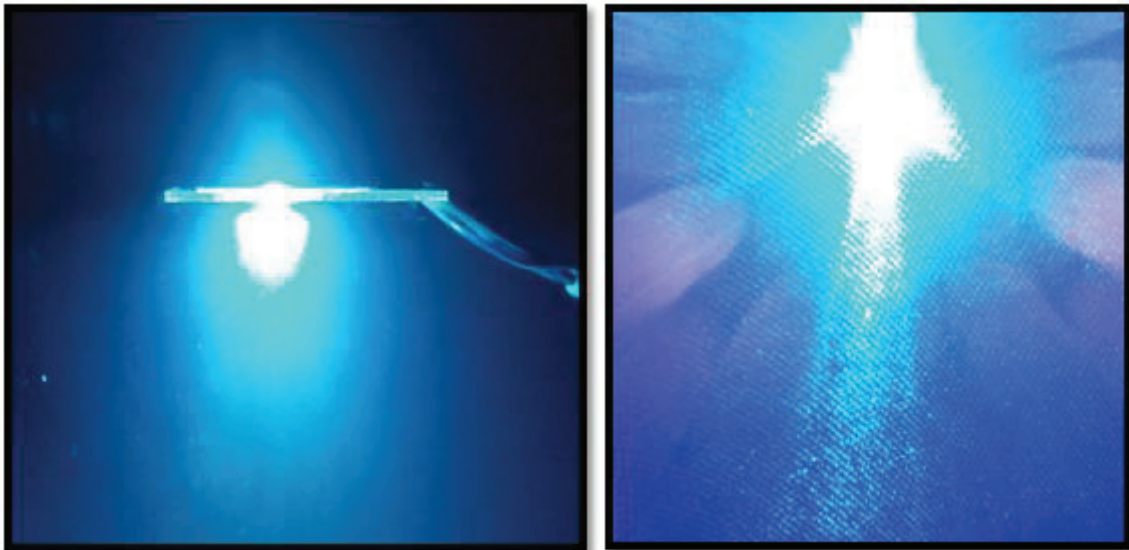
Figure 4.2 Left: OLED operating in pulsed mode, Right: Commercial LED in the pulsed mode

LED Light Collimating System:

Since, organic light emitting diodes, under study in this thesis have an optical intensity of ~1mW/mm^2 at 14V pulsed mode operation, and is likely to burn out upon using it at a higher intensity, an optimum design for coupling this light source to an optical fiber has been designed.

According to the model used by (Aravanis, et al., 2007), if the incident light intensity is I(0), the effective intensity of light after reflection and dispersion of light due to the brain tissue at a depth of I(z) is given by:

$$\frac{I(z)}{I(z=0)} = \frac{\rho^2}{(Sz+1)(z+\rho)^2}$$

Where S is scatter coefficient (for mouse estimated to be 11.2 mm^{-1}) and ρ is,

$$\rho = r\sqrt{\left(\frac{n}{NA}\right)^2 - 1}$$

Here, r is the radius of optical fiber (light source), NA is the numerical aperture of the optical fiber, and n (1.36, (T, 2003)) is the refractive index of the brain. The only parameter remaining to be found for the OLED light source is its equivalent numerical aperture.

z /rho = 2.404

By definition, Numerical Aperture is a unitless number characteristic of the range of angles over which it can emit or accept light, depends on the half angle in the media. As shown in the Figure 4.3, it can be numerically described to be:
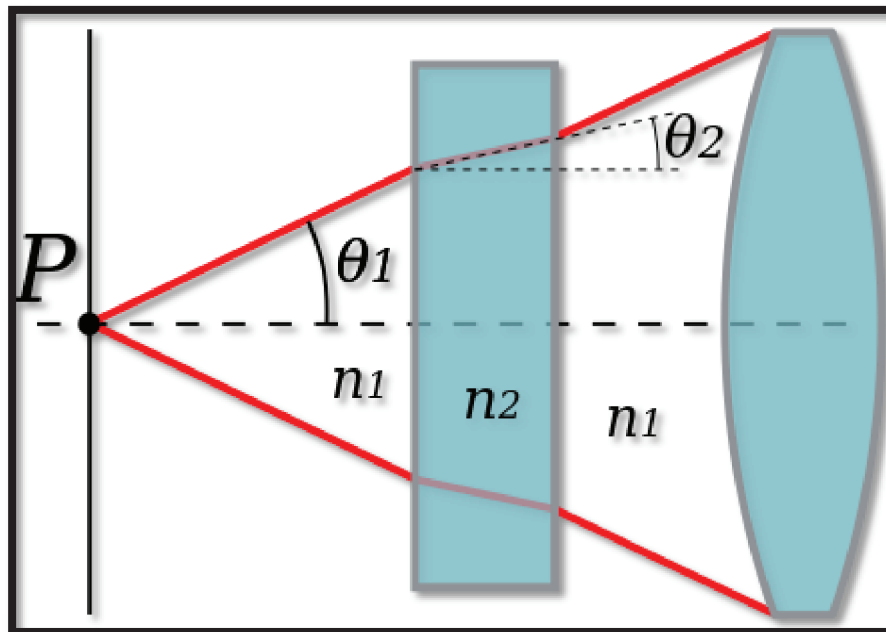
Figure 4.3 By the definition Numerical Aperture is a number = **n1 sin θ1 = n2 sin θ2** (Alexandrov, n.d.)

Hence for the OLED light source in the air media, we can make a crude estimate of its numerical aperture from the light distribution in the Figure 4.5. The half angle is 70°. Hence the NA = 1*$\sin 70° = 0.77$

Plugging $NA = 0.77, n = 1.36, r = 200um$ into the above equation of intensity at depth $z = 700um$, gives $I(700um) = 0.097 * I(0)$.
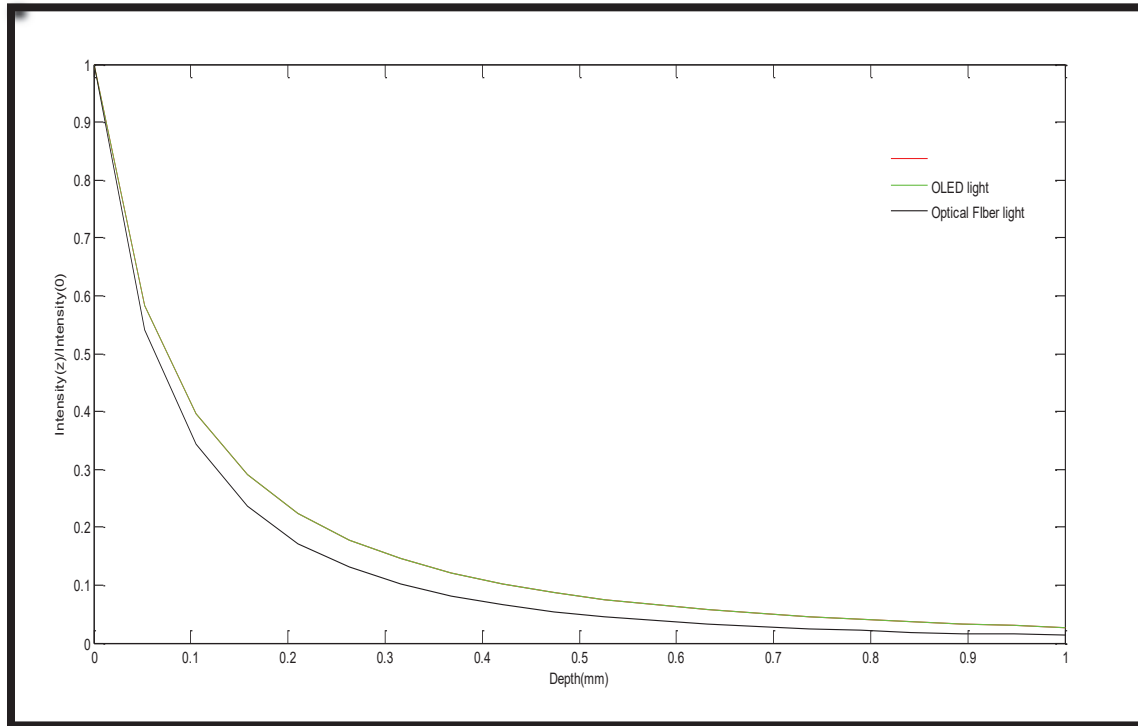
Figure 4.4 OLED and Optical Fiber, light intensity ratio at depth z

For this reason given by our discussion in chapter 2 on the kinetics of the Channel Rhodopsin, the light gated channel at the depth of 700um should not open.

The array of possibilities with the OLEDs for optogenetics in the future is immense. As part of this study, and the stage that the OLED technology stands, it is imperative to conclusively show if the OLEDs if kept next to the neurons can stimulate the neurons. For this reason, an optical system was custom designed to couple the LED light into optical fiber with as much efficiency as possible.

LED To Optical Fiber Coupling System:

The literature suggests 3 key methods for coupling the LED light to the optical fibers (Optics, n.d.). First is to utilize infinity corrected microscope objectives in retro position; this works well but is by far the most expensive solution. Second option is to use fiber optic collimator/ focuser assemblies, available with an SMA connector. You can achieve spot sizes of a few microns. This technique offers the most value for the expense. Another technique can use ball lenses; this the least expensive solution. When coupling light from a LED into a fiber, the choice of ball lens is dependent on the Numerical Aperture (NA) of the fiber and the LED's spot diameter. The LED's spot diameter is used to determine the NA of the ball lens. The Numerical Aperture of the ball lens(light emitter), should be less than the NA of optical fiber(light accepter).

The current commerically available optogenetic light source(Thorlabs) setup consists of Optical Fiber in a cannula, coupled with a patch cable . The patch cable has a standard SMA connector via which it is connected to the LED light source.

Keeping in mind the suggestions from the literature for coupling LED light to optical fiber, the fiber coupled LED Light Source was replaced in the figure 4.6 was replaced by a custom designed lens-collimator for coupling as much light as possible from the flat LED light
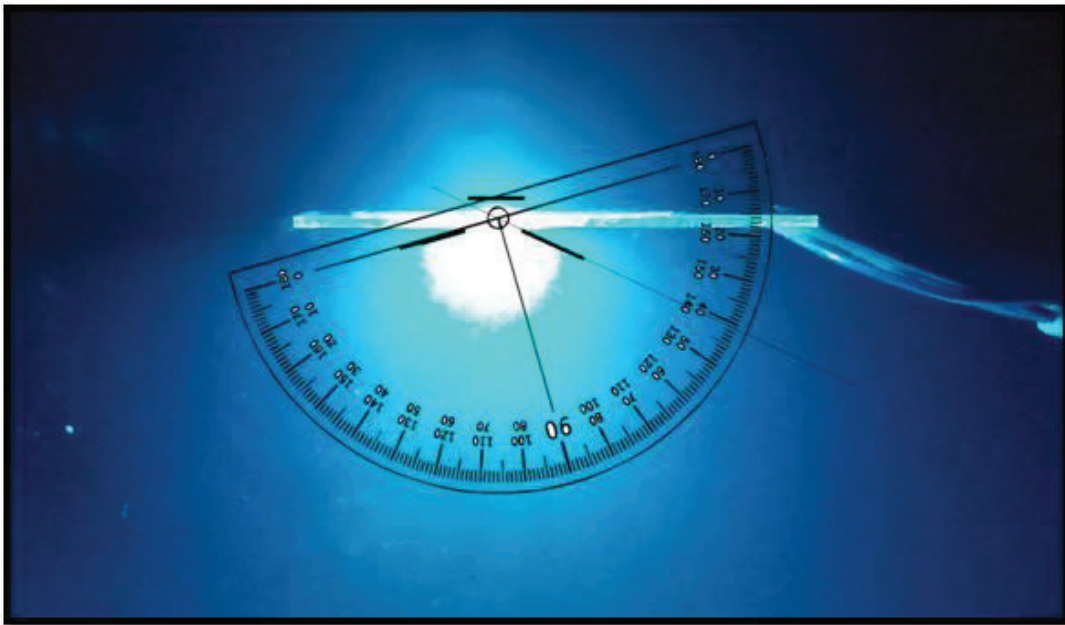
Figure 4.5 Light spread measurement

source(OLED) into the same fiber optic cannula via the fiber optic patch cable. The key

components of the system as are shown in Figure 4.7.
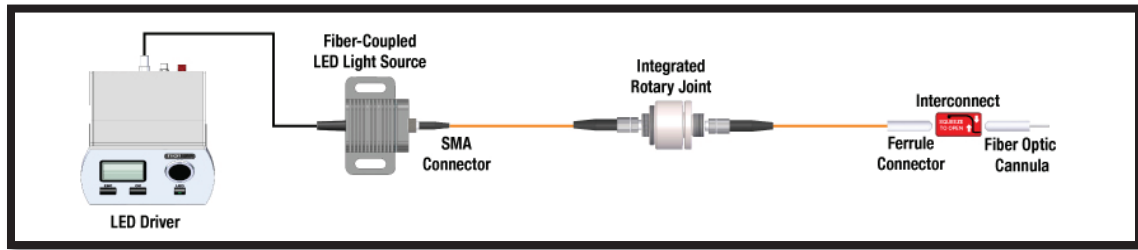
Figure 4.6 Commercial Optogenetic Light Sourcing setup (Thorlabs)
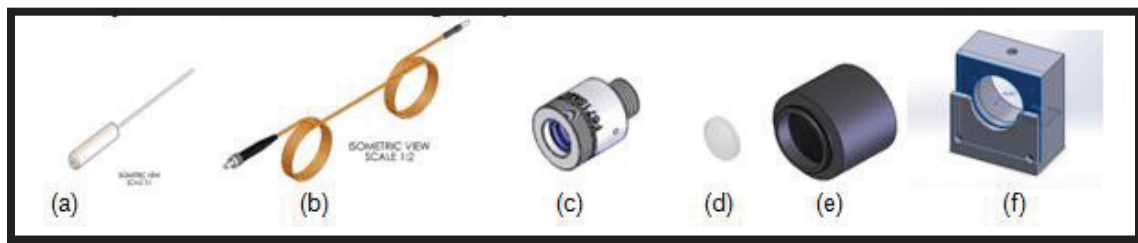
Figure 4. 7 Custom designed LED light to Optical fiber coupling system (a) Fiber optic cannula (b) Fiber Optic patch cable - has a standard SMA connector and fits into the collimator (c) Collimator connects to the SMA connector on one side and to the SM05 lens tube on the other side (d) lenses are positioned inside the lens tube (e) SM05 lens tube (f) A 3D printed stand for the OLED flat light source to stably couple the light into the collimating system

The assembly of the lenses was decied based on the simulation of a bunch of cases on

Optical Ray Tracer, an open source Optical simulation software.

The internal lining of the lens tube was considered to be reflective in the simulation as the actual

lens tube internal area was covered with mylar coated aluminium oxide film which is 98%

reflective.

Simulation results of 3 different cases are shown in the figure 4.8-4.10. The planoconvex

lenses and the biconvex lens features have been adopted from thorlabs datasheet for the

corresponding lenses bought. The lens towards the extreme right in all the 3 cases is

representative of the collimator's lens. The dimensions for the same have also been adopted from

the datasheet available for the collimator. Clearly the case 3, disperses the light rather than

focusing it. Ideally, it is required to collect all the light and focus it on the focal point of the lens

towards the right. The optical fiber at that location should have a Numerical Aperture enough to

accept most of the light getting focused on the focal point. Due to several uncertainties, it will be

better to have as high a numerical aperture as possible for the optical fiber connecting to the focal point of the lens. The optical fiber is located at the focal point of the collimator via the SMA connector of the fiberoptic patch cable.
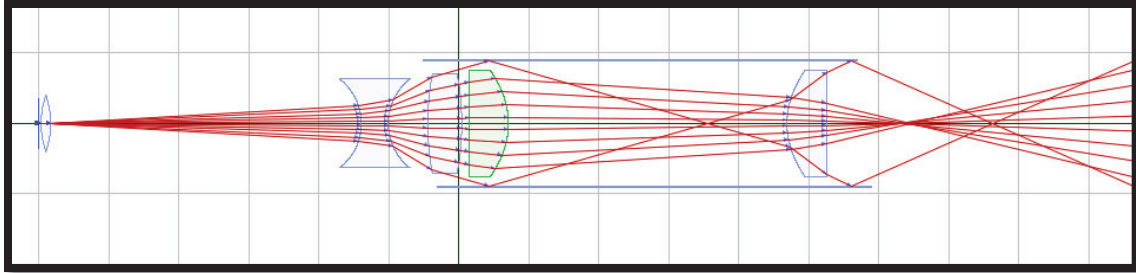
Figure 4.8 Case: Using both lenses adjacent:
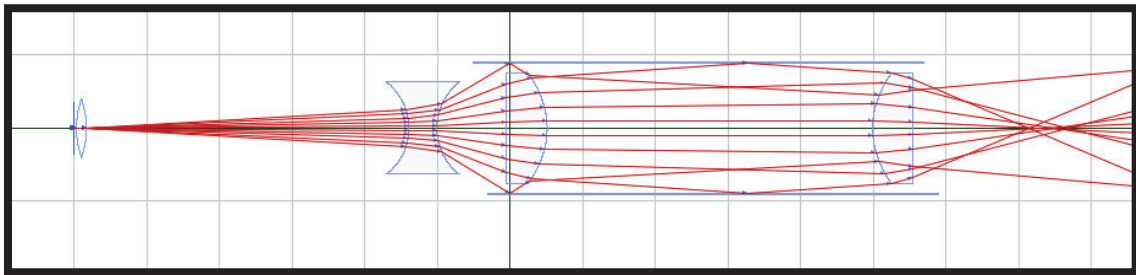
Figure 4.9 Case: With the plano convex lens, next to the light source
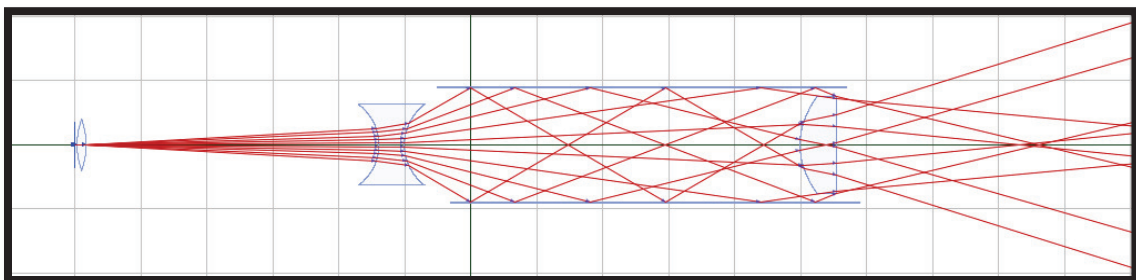
Figure 4.10 Case: No lenses in the lens tube

The figure 4.11 shows the visual inspection results of the coupling of the LED to the optical fiber. The fiber optic patch cable and the fiber optic cannula with optical fiber of $\emptyset 400um$ were chosen because the, collimators spot diameter is expected to be imperfect, and it is ideally required that all the photons at the focal point be collected into the optical fiber as possible and source to the neuron via the fiber optic cannula.
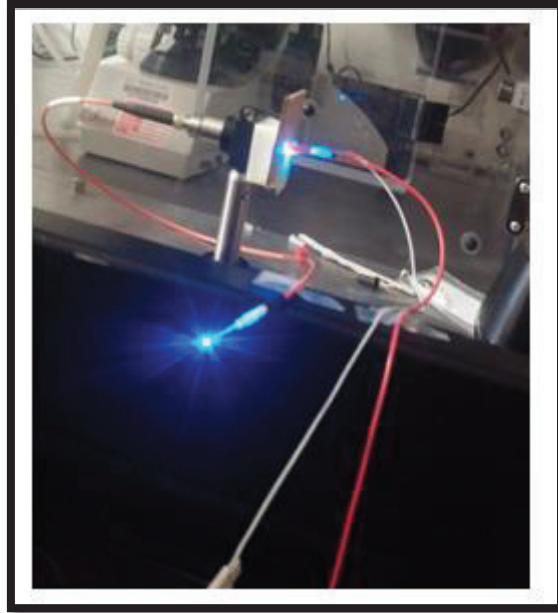
Figure 4.11 Commercial LED response through the system.

Figure 4.12 Optoscope Reading: Left: Baseline, Middle: Direct coupling of led, Right: led coupled to the Optical System

To get an estimate of the coupling efficiency of the LED to the optical fiber, a

TEKTRONIK 2715 Optoscope was used. As shown in the Figure 4.11, baseline activity was

recorded keeping the optical input of the scope open. 1 division on the vertical axis corresponds

to ~90µW. To measure the intensity as sensed by the optoscope for the bare LED, the LED stuck

directly into the input port of the Optoscope (Figure 4.12, middle). As seen in the image the

intensity recorded is ~420µW. Upon plugging the LED to the optical collimating system and using

a 65um SMA connector fiber optic patch cable, the reading of the Optoscope is ~90uW. Hence an estimate of 21.5% efficiency is reported for the LED to Optical Fiber coupling system.

The literature shows upto -4dB(~35%) Gain in the efficiency of LED to optical fiber coupling through a lens system (Wetzel, 1993).

ICMS Electrode Design

When glass micropipette is used, with the tip dimension of $5um$, and impedance of $1M\Omega$, a current of $20-60uA$ is enough to evoke visible response when stimulated in the M1 motor cortex. It has been concluded it is the current density which is of essence in depolarizing the neurons by inducing current. The FHC Tungsten microwires used, did have an impedance of $1M\Omega$,(Figure 4.13, Electrode Impedance Spectrogram, CH Instruments) but the exposed tip was $30um$ long with a 2um tip.
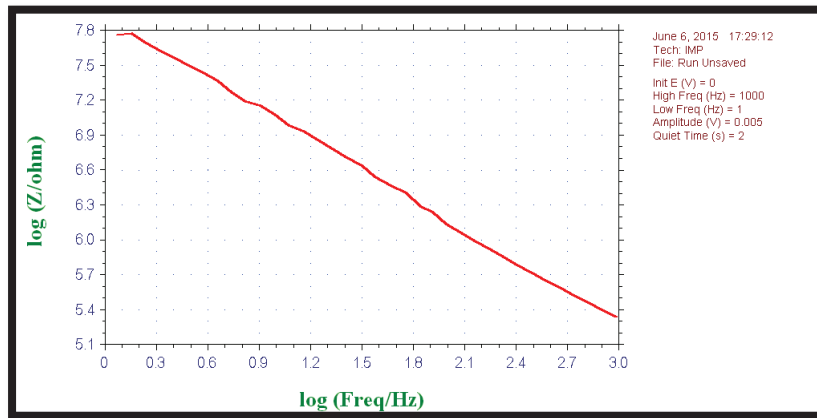
Figure 4.13 FHC Tungsten Microwire Electrode Impedance Spectrum

As shall be seen in the response curves, the least required currents to get region specific response from the neurons was $200uA$ both in the Rat and Mouse experiments. It is necessary that the power source can source the Power = (Current)*(Electrode Tissue impedance).

EMG Electrode Placement

Uncoated stainless steel 60um AM Systems wires were utilized to acquire EMG signals. 2 wires were inserted to the muscle group of interest and 1 wire was slid underneath the skin but not into

the muscle. Intan Amplifier board was used for the purpose of acquisition of EMG signals. For the analog amplifier lower cut-off frequency was programmed at 10Hz and higher cut-off frequency was set at 1000Hz. The notch filter at 60Hz was operational.

The 60um wires were implanted into the muscles using 26 Gauge needle as a guide. Once inside, the leg along with the wire was held and the needle taken out to leave the wire inside the muscle. The wires were implanted in the vastus lateralis or quadriceps muscle groups.

ICMS Experiments

Since the lead time on the delivery of transgenic animals was around 3 months and neocortical stimulation of neurons was hypothesized to not very likely evoke limb movement, an optical fiber of 400um diameter was to be placed next to the pyramidal layer V neurons. The experimental protocol has to be established on control animals. In addition to the surgical procedure, the ICMS electrode design is critical to deciding the normal stimulation parameters. The discussion on the ICMS electrode design is in the previous section

The experimental setup consisted of the stereotaxic frame, with earbars to hold the mouse on, a nose cap for supplying the oxygen and isoflourance mix, current source, voltage source, LED Driver, intan amplifier connected to the computer for recording the event and the EMG signals in real time.

4.3 Results

Rat Control Data

The stimulus parameters for the ICMS experiments consisted of 14 pulses in a train, each 200us 'ON' time, and separated by 2.86ms. The pulse train goes on for 40ms(These 40ms are indicated by the red trace in Figure 4.14-4.16). The next pulse train is delivered 1 second after. (Young, Vuong, Flynn, & Teskey, 2011)
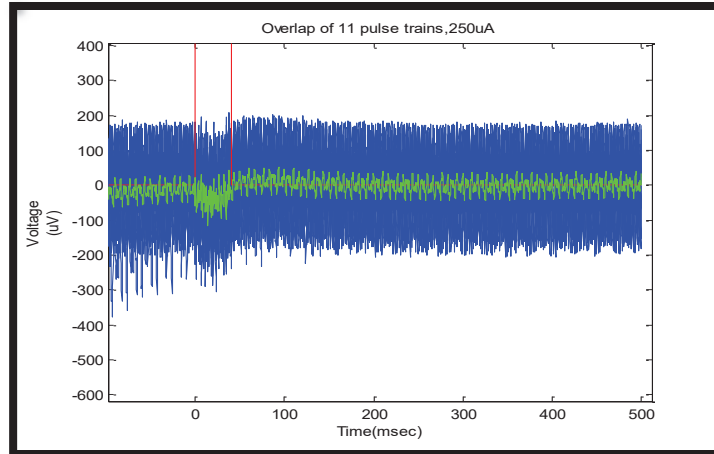
Figure 4.14 EMG Response, M1 region motor cortex stimulation contralateral hind limb response
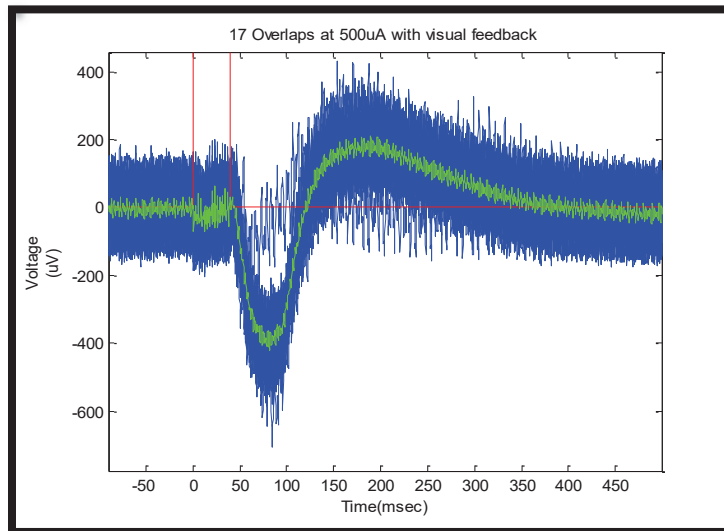
Figure 4.15 EMG Response, M1 region motor cortex stimulation contralateral hind limb response

Figure 4.14 shows the time aligned EMG response curves. It can be seen that shortly after the stimulus begins(~10ms) there is a consistent increase in the EMG amplitude response. There was no response below 200uA. In the Figure 4.15, a very clear EMG response begins shortly(~10ms) after the onset of the electrical stimulation. As seen in the Figure 4.14, when the stimulus is at the forelimb region of the motor cortex there is no visual response in the hindlimb, also there is no characteristic EMG response 10ms after the onset of the electrical stimulation. At this time visual forelimb response was noted.

36
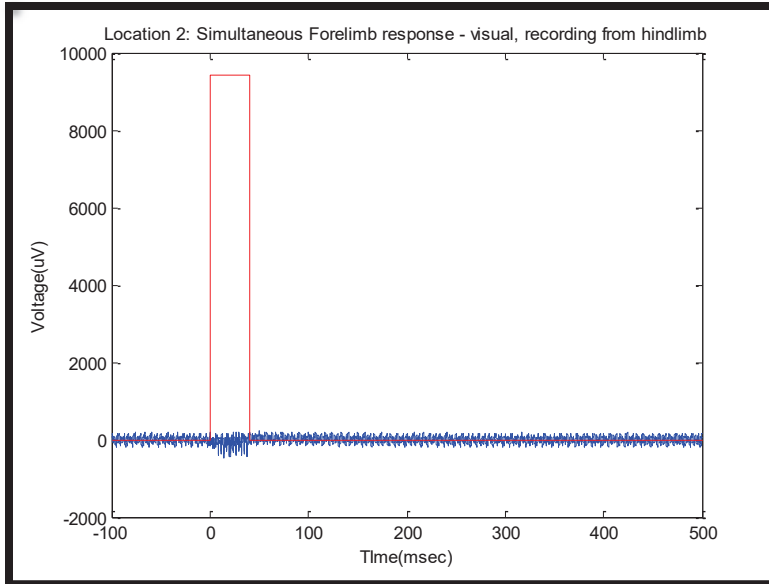
Figure 4.16 EMG recording from contralateral hind limb recording, when forelimb motor cortex region stimulated

Mouse Control Data:

Mouse stimulus parameters were similar to the rat experiment with14 pulses in a train, each 200us 'ON' time, and separated by 2.86ms. The pulse train goes on for 40ms. The next pulse train is delivered 1 second after. Red traces in the Figure 4.17-4.19 show the 13 pulses in the 40ms duration.
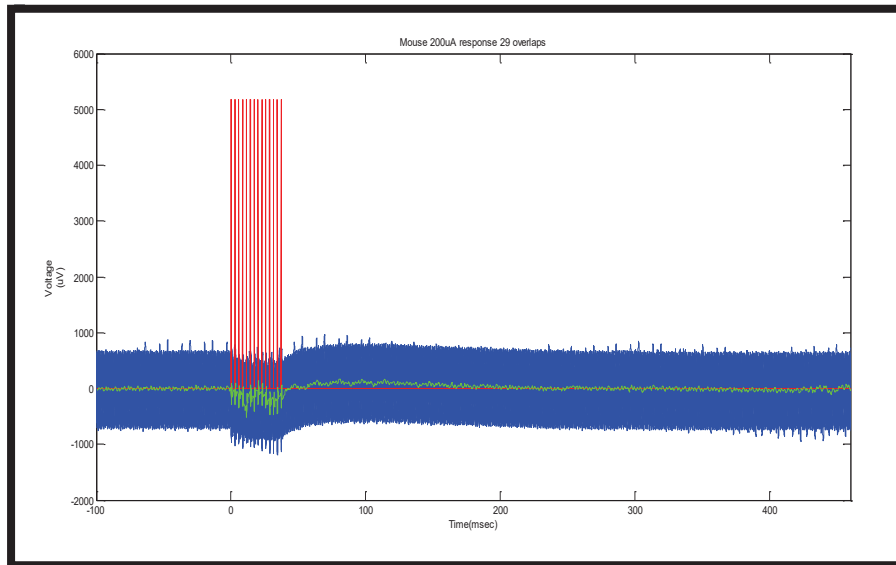
Figure 4.17 200uA Pulse train, Hindlimb EMG response
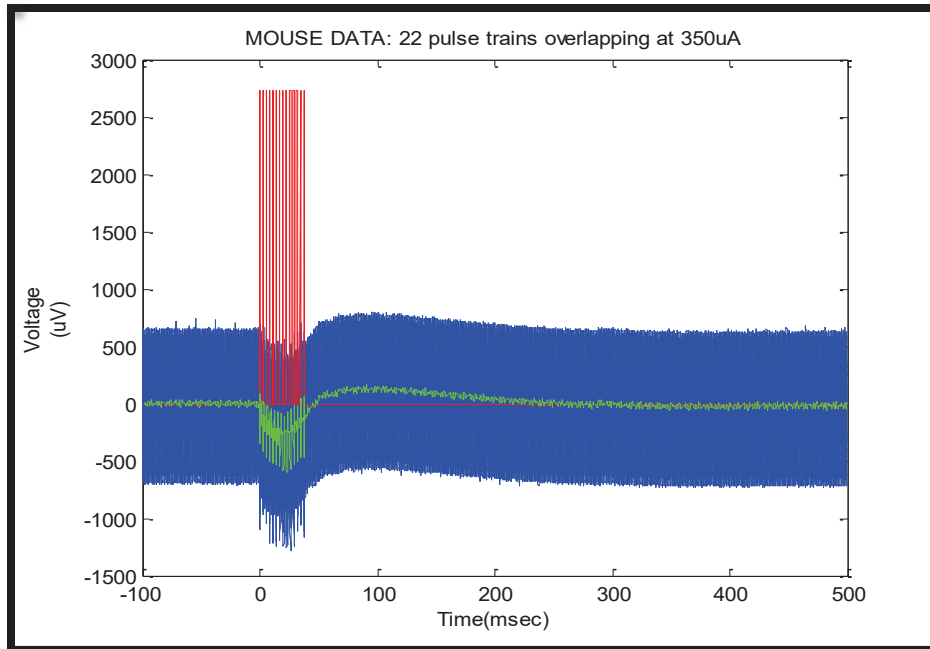
Figure 4.18 350uA pulse train, Hindlimb EMG response
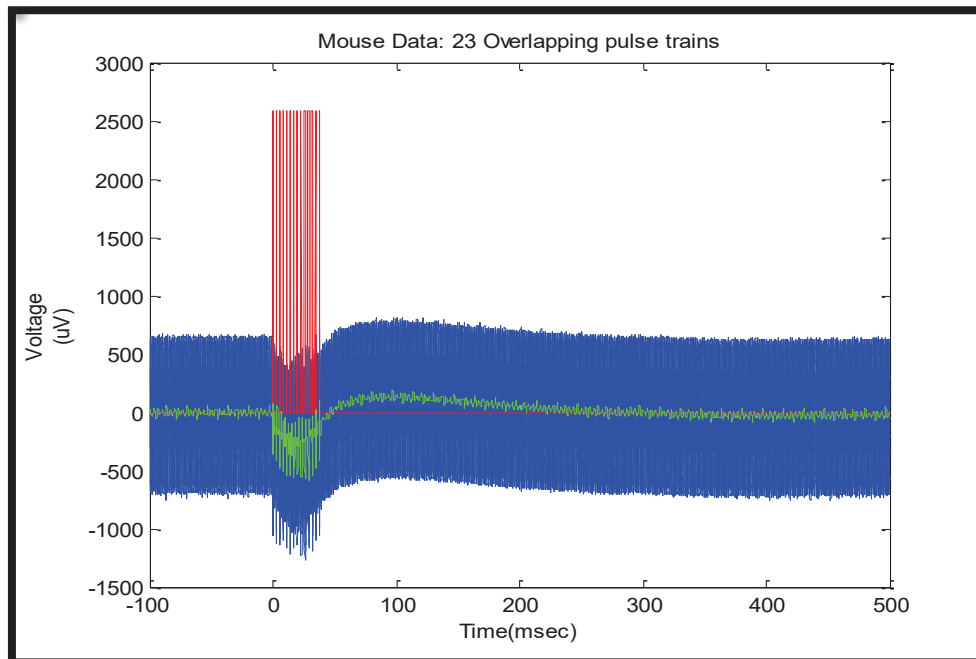
Figure 4. 19 400uA Pulse train, Hindlimb EMG response

Figure 4.17-4.19(at 200μA, 350μA, 400μA respectively) show EMG response evoked due

to the electrical stimulus. Since there is a ~10ms delay in the response amplitude change, the

response is noted to be actually EMG response. Video responses of hind limb has also been
noted.
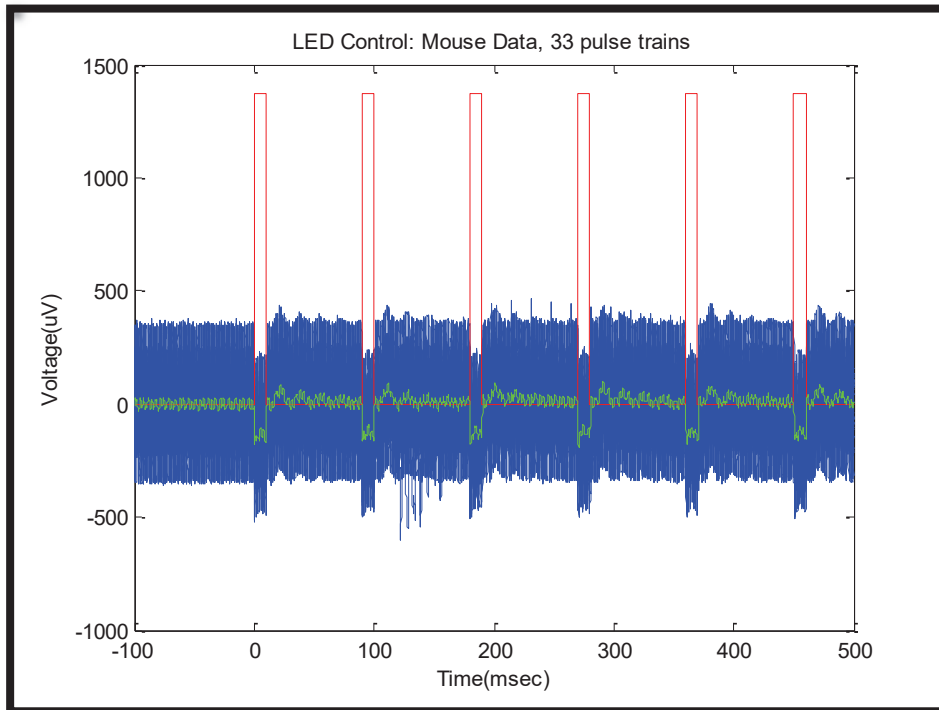
Figure 4.20 Control LED Response, only time synchronized capacitive noise
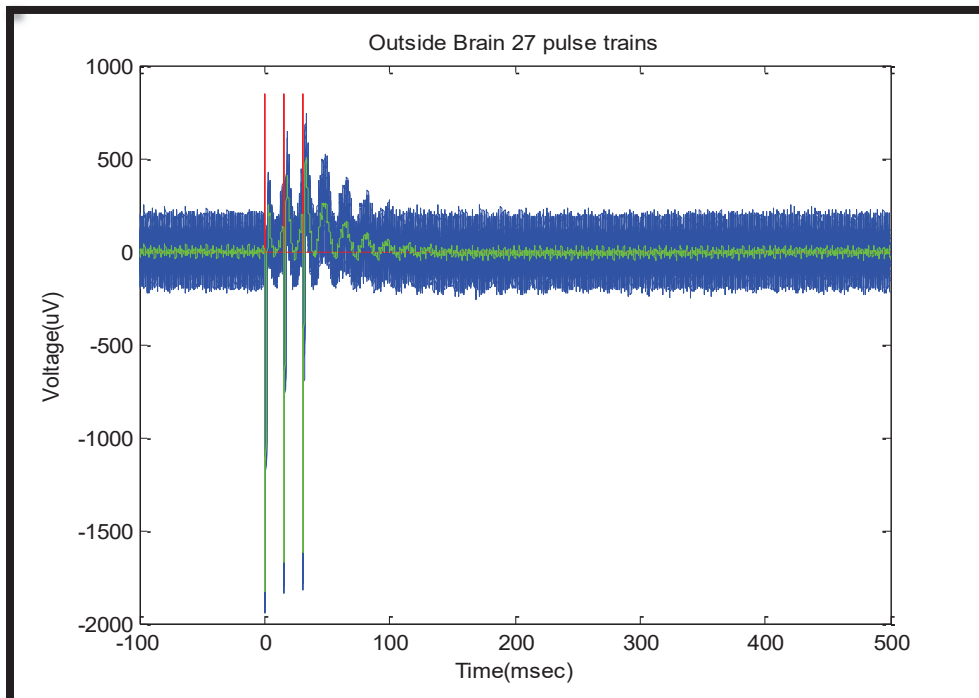
Figure 4.21 Outside Brain, characteristic noise - Capacitive coupling

On the other hand, in Figure 4.21, control experiment with the commercially available LED was conducted. A very time correlated, capacitively coupled artifact was noted. In the Figure 4.19, ICMS response from EMG, when the electrode is kept outside the brain is taken. The EMG response shape is again highly time correlated which indicates it is capacitively coupled artifact and not muscle activity

Transgenic Mouse Data

Successful hind limb and tail twitching were evoked in n=2 mice using the iLED. The OLEDs could not evoke a similar response. Videos of n=2 cases of tail movements were recorded. There was no EMG activity for the response which was recorded. This means that the layer 5 pyramidal neurons were not stimulated. It should be noted that EMG electrodes where inserted had a significant amount of fat deposited over the muscle due to aging.

Neither the OLED nor the iLEDs could evoke any activity(tail or hind limb movement), using the optical fiber. A significant capacitive coupled noise is seen similar to the control experiment. This appears worst since the operational frequency and number of pulses have been decreased.
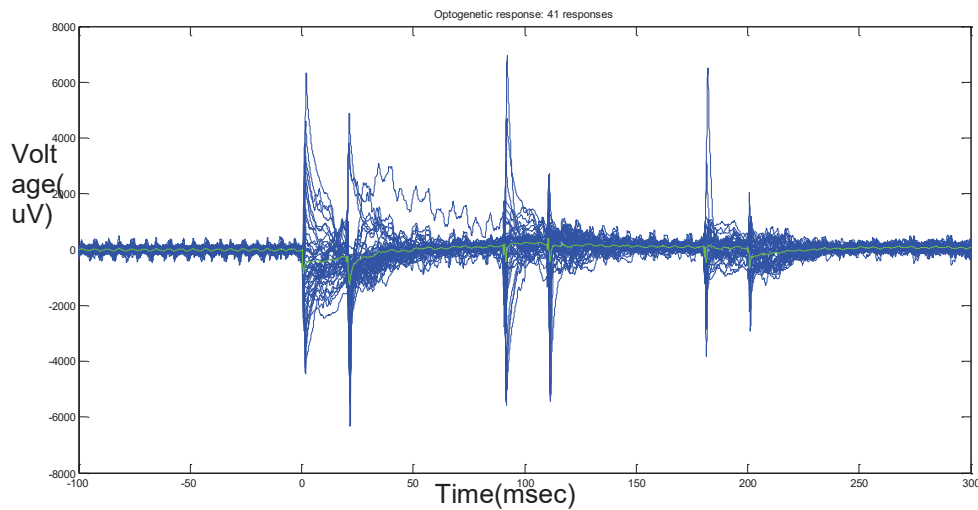
Figure 4.42 Transgenic mouse direct iLED stimulation – 41 pulse trains time aligned
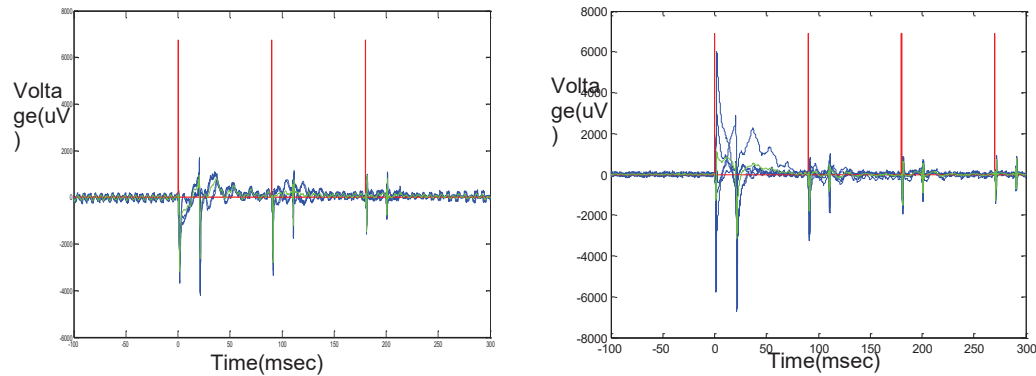
Figure 4.23 (Left) iLED optical fiber (Right) OLED optical fiber - stimulation parameter changed

4.4 Discussion

As the FHC microwires were 30μm uninsulated, current densities of 20-60uA are too little to depolarize the neurons in the surrounding region. A large chunk of neurons will be thrown at with charge due to a larger surface area. Hence the requirement of higher current levels is due to the higher uninsulated area.

The positioning of the EMG electrodes in Rat animal model is convenient, but for the mouse animal model the electrode needs to be implanted carefully into the muscle since the muscle groups are quite smaller. Care should be taken to make sure that both the wires coming out of the muscle are in similar physical situation(both touching or not touching the surroundings here or skin) for efficient Common Mode noise removal. If one wire coming out touches the skin and the other does not then noise will be introduced into the signal.

Both the rat and the mouse control data suggests two key points. Firstly, if the response of the EMG is delayed by 10ms from the time of stimulus, then the response is actually due to the evoked response in the muscles. In the control data (outside brain stimulation, non-hindlimb motor cortex region stimulation, and LED stimulation), the response is very time synchronous. This can act as a quantitative measure to predict the response is evoked or is noise.   Secondly, beyond a current threshold value in a certain range (Figure 4.16, 4.17), the evoked EMG response is similar irrespective of the current level. This is because once the Layer V pyramidal neurons depolarize, it causes the other evoked motor response after the requisite synapses.

Supplementary video (Optogenetic stimulation), shows a sustained tail movement response to commercial LED operating in pulsatile mode. When the light is blocked the tail movement stops and vice-versa. Operating intensity in the pulsed mode of the commercial LED ~2mW/mm^2. Similar responses could not be evoked neither using OLED, nor using optical fiber coupled with iLED or OLED.

From Figure 4.22, it can be observed that the noise levels have decreased. This likely because of the increase in the distance between the leads to the LED(since the light source is now behind the optical system).

CHAPTER 5

CONCLUSIONS AND FUTURE DIRECTIONS

In the experiments performed so far OLEDs have consistenly worked in in vitro conditions (2 separate experiments, multiple trials). For the chosen experimental design they have not worked in-vivo so far. iLEDs can show response in vivo when operated 5-6 V in pulsed mode. OLEDs cannot stimulate the pyramidal neurons, but if placed next to the neuron it could possibly stimulate them (hypothesis based on the in vitro result).

In the Figure 5.1 is shown an initial experimental setup. Here the Optical Fiber setup described earlier is used to source the OLED light through the optical fiber at an angle. The optical fiber is to be slid into the brain. Simultaneous spontaneous and optically modulated neuronal activity is to be recorded. The optical fiber may be replaced by direct LED stimulation neocortically. Since the blue OLED could not stimulate the deeper pyramidal neurons, strategies similar to this one are being developed to modulate neurons at an upper level than the Layer V.

Red shifting genes and hyperpolarizing genes could potentially make the OLEDs more useful at the current state of art of the technology.
Experiments for green light maybe shown to be useful by transfecting neurons with C1V1tt. For the purpose neurons ~10 DIV should be co-transfected with C1V1tt and CAG-cre.

Optogenetic neural silencing of neurons by transfecting primary cortical neurons with eMAC3.0 hyperpolarizing green light sensitive Opsin may be explored but a significant amount of work still needs to be pursued for readying the hardware. This system has the functionality to electrically stimulate neurons at 2 electrode locations and record from the rest. Efforts have been made in making a custom parallel electrical stimulus and optical silencing system. Parallel efforts in utilizing TDT stimulation recording system is also underway in the lab.
Given, the ability of the technology to be fabricated monolithically, along with the electronics, in extremely thin micron to submicron scale, its utility in modulating neocortical neurons is pronounced.   The OLED technology despite so many ups, faces some key challenges. Firstly, the maximum intensity obtained reliably without burning the blue OLEDs is 1mW/mm^2, perhaps a little more for green OLEDs and the more red-shifting OLEDs. Given the fact that the light

intensities drop significantly while propagating through the tissue due to absorption and scattering, very high intensity light sources are required. The discovery of red shifting, highly sensitive light gated Opsins for hyperpolarizing and depolarizing the neurons can aide in the utility of OLEDs.
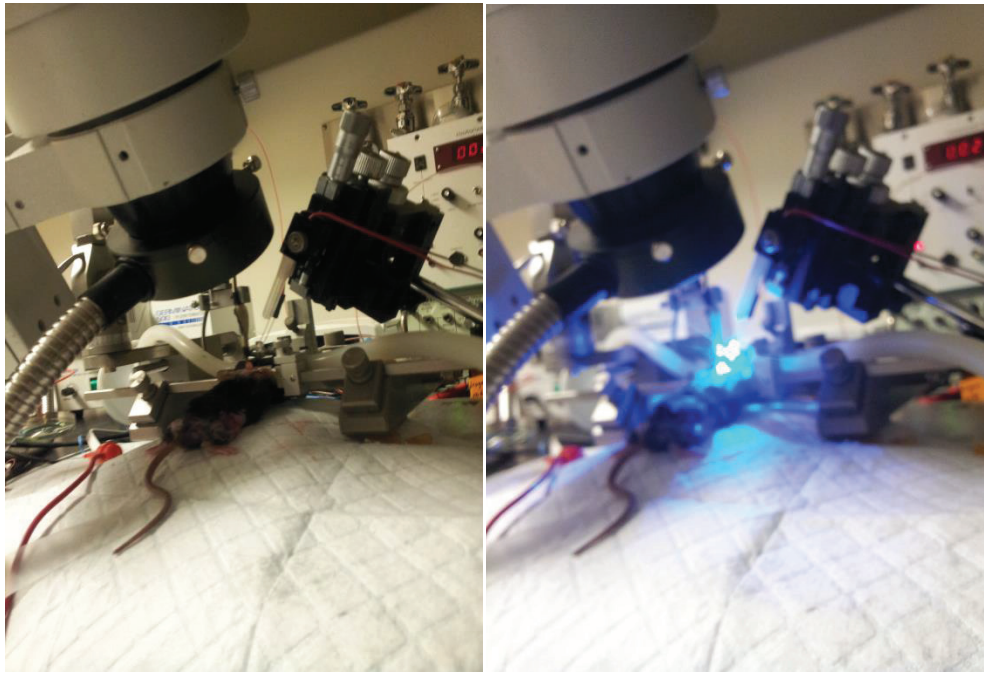

Figure 5.1 Optical stimulation and neuronal recording setup

The second challenge, which is perhaps only currently an issue is that of low shelf life of the OLEDs. Because of their Organic layer, the degradation of the OLED is faster. This could perhaps be solved faster with design of clever encapsulation to limit the interaction of the Organic Layer with the atmosphere.

.

REFERENCES

Boyden ES, Z. F. (2005). Millisecond-timescale, genetically targeted optical control of neural activity. Nat Neurosci., 1263-8.

Abaya, T., Blair, S., Tathireddy, P., Rieth, L., & Solzbacher, F. (2012). A 3D glass optrode array for optical neural stimulation. Biomedical Optics Express,, 3087-04.

Alexandrov, O. (n.d.). Numerical Aperture. Retrieved from https://en.wikipedia.org: https://en.wikipedia.org/wiki/Numerical_aperture#/media/File:Numerical_aperture.svg

Anikeeva, P. (2013). Flexible Optoelectronic Devices for Neural Recording and Stimulation. NAE USFOE.

Anthony N. Zorzos, J. S. (2012). Three-dimensional multiwaveguide probe array for light delivery to distributed brain circuits. Opt. Lett., 4841-43.

Aravanis AM, A. A. (2007). Neural substrates of awakening probed with optogenetic control of hypocretin neurons. Nature.

Aravanis, A. M., Wang, L.-P., Zhang, F., Meltzer, L. A., Mogri, M. Z., Schneider, M. B., & Deisseroth, K. (2007). An optical neural interface: in vivo control of rodent motor cortex with integrated fiberoptic and optogenetic technology. Journal of Neural Engineering, , 143-56.

Deiseroth, K. (2011). Optogenetics. Nature Methods, 26-29.

G. Raupp, S. O. (n.d.). Low Temeprature Amorphous Silicon Backplane technology development for Flexible Display in a Manufacturing Pilot line environment. JSID, 15(7), 445-454.

Gregory B. Raupp*, S. M. (2012). Low-temperature amorphous-silicon backplane technology development for flexible displays in a manufacturing pilot-line environment. Society for Informaton Display, 445-454.

Iwai Y, H. S. (2011). A simple head-mountable LED device for chronic stimulation of optogenetic molecules in freely moving mice. Neurosci Res.

Kim, T.-I., McCall, J. G., Jung, Y. H., Huang, X., Siuda, E. R., Li, Y., . . . Tan, M. P. (2013). Injectable, cellular-scale optoelectronics with applications for wireless optogenetics. Science, 211-216.

Marrs, M., Moyer, C., Bawolek, E., & Cordova, R. (2011). Control of Threshold Voltage and Saturation Mobility Using Dual-Active-Layer Device Based on Amorphous Mixed Metal– Oxide–Semiconductor on Flexible Plastic Substrates. Electron Devices, IEEE Transactions on , 3428-34.

Matsuda T, C. C. (2007). Controlled expression of transgenes introduced by in vivo electroporation. Proc Natl Acad Sci U S A.

Mattis, J., Tye, K. M., Ferenczi, E. A., Ramakrishnan, C., O'Shea, D. J., Prakash, R., . . . Deisseroth, K. (2012). Principles for applying optogenetic tools derived from direct comparative analysis of microbial opsins. Nature Methods, 159-72.

McCall, J., Kim, T., Shin, G., Huang, X., Jung, Y., Al-Hasani, R., . . . Rogers, J. (2013). Fabrication and application of flexible, multimodal light-emitting devices for wireless optogenetics. NATURE PROTOCOLS,, 2413-28.

Optics, E. (n.d.). Frequently Asked Questions. Retrieved from www.edmundoptics.com: http://www.edmundoptics.com/technical-resources-center/frequently-asked-questions/index.cfm?categoryid=19

Pashaie, R., Anikeeva, P., Lee, J. H., Prakash, R., Yizhar, O., Prigge, M., . . . Williams, J. (2014). Optogenetic Brain Interfaces. IEEE Reviews in Biomedical Engineering,, 3-30.

Patel and J., M. C. (2012). High efficiency, Site-specific transfection of adherent cells with siRNA using microelectrode arrays. Journal of Visualized Experiments(67).

Pisanello, F., Sileo, L., Oldenburg, I., Pisanello, M., Martiradonna, L., Assad, J., . . . De Vittorio, M. (2014). Multipoint-Emitting Optical Fibers for Spatially Addressable In Vivo Optogenetics. Neuron, 1245-54.

Prigge, M., Schneider, F., Tsunoda, S. P., Shilyansky, C., Wietek, J., Deisseroth, K., & Hegemann, P. (2012). Color-tuned channelrhodopsins for multiwavelength optogenetics. J.Biol.Chem., , 31804-12.

Pronichev, I. V., & Lenkov, D. N. (1998). Functional mapping of the motor cortex of the white mouse by a microstimulation method. Neurosci.Behav.Physiol., 80-85.

Roome CJ, K. B. (2014). Chronic cranial window with access port for repeated cellular manipulations, drug application, and electrophysiology. Frontiers in cellular neuroscience.

Royer, S., Zemelman, B. V., Barbic, M., Losonczy, A., Buzsáki, G., & Magee, J. C. (2010). Multi-array silicon probes with integrated optical fibers: Light-assisted perturbation and recording of local neural circuits in the behaving animal. Eur.J.Neurosci., , 2279-91.

Samuel, L. (n.d.). http://www.interactive-biology.com/49/proteins-in-the-membrane-of-the-neuron-and-their-functions/. Retrieved from http://www.interactive-biology.com.

Schwaerzle, Albert-Ludwigs, Elmlinger, P., Paul, O., & Ruther, P. (2014). Miniaturized Tool for Optogenetics Based on an LED and an Optical Fiber Interfaced by a Silicon Housing. Engineering in Medicine and Biology Society (EMBC), 2014 36th Annual International Conference of the IEEE, 5252-5255.

Smith, J., O'Brien, B., Lee, Y.-K., & Bawolek, E. (2014). Application of Flexible OLED Display Technology for Electro-Optical Stimulation and/or Silencing of Neural Activity. Journal of Display Technology, 514-20.

Smith, J., O'Brien, B., Lee, Y.-K., & Bawolek, E. (2014). Application of Flexible OLED Display Technology for Electro-Optical Stimulation and/or Silencing of Neural Activity. Journal of Display Technology, 514-20.

T, V.-D. (2003). Biomedical Photonics Handbook. Raton, FL: CRC Press.

Tae-il Kim, J. G.-H. (2013). Injectable, Cellular-Scale Optoelectronics with Applications for Wireless Optogenetics. Science, 340.

Wetzel, S. (1993). Coupling light emitting diodes to multimode optical fibers. Lehigh University.

Yizhar O, F. L. (2011). Neocortical excitation/inhibition balance in information processing and social dysfunction. Nature., 171-8.

Young, N. A., Vuong, J., Flynn, C., & Teskey, G. (2011). Optimal parameters for microstimulation derived forelimb movement thresholds and motor maps in rats and mice. J.Neurosci.Methods,, 60-69.

APPENDIX A

MATLAB CODE FOR MAKING THE BOX PLOTS, COLLECTING WAVESHAPES, AND

AVERAGING THEM

```matlab
%% Code to see the entire data, when recorded using Intan Amplifier
clear
read_Intan_RHD2000_file;
figure,
plot(t_amplifier,amplifier_data(1,:),'b');
hold on
y=board_dig_in_data*max(amplifier_data(1,:));
plot(t_dig,y,'r');

%%Code for Overlapping the time synchronus activity in the invivo
%%experiments:
close all;
clear
read_Intan_RHD2000_file;
figure,
plot(t_amplifier,amplifier_data(1,:),'b');
hold on
y=board_dig_in_data*max(amplifier_data(1,:));
plot(t_dig,y,'r');

y=board_dig_in_data*max(amplifier_data(1,:));
check=y(1,2:end)-y(1,1:end-1);
K=find(check>0);
initial=[];
B=K(K>2000);
initial=B(1);
% initial(1)=K(1);
for i=K(1:end-1)
    if i>(initial(end)+18000)
        initial(end+1)=i;
    end
end
m=linspace(-100,500,20*600);
figure,
for k=initial
    plot(m,amplifier_data(1,k-(100*20)+1:k+(500*20)));
    hold on;
end
plot(m,y(1,(initial(1)-(100*20)+1):initial+(500*20)),'r');
f=1;
for k1=initial
%     plot(m,amplifier_data(1,k-(20*20)+1:k+(100*20)));
M(f,:)=amplifier_data(1,(k1-(100*20)+1):k1+(500*20));
f=f+1;
end
% M(f,:)=amplifier_data(1,k-(20*20*5)+1:k+(100*20*5));
B1=mean(M,1);
hold on;
plot(m,B1,'g');
```

%% code for box plots and performing the student's t-test

```
function[t_test_result]=boxplot_t_test(data,alpha_val)
%data: trial X data
boxplot(data,'labels',{'pre-stimulus','during-stimulus','post-
stimulus'});%% should have trial x data
t_test_result =
ttest2([data(:,1);data(:,3)],data(:,2),'Aplha',alpha_val);
end
```

%%calling the above function with the data for spikes rates for n number of trials

 %%arranged in the rows and 1st column for prestimulus spike rates, 2nd for during

%%stimulus spike rate and 3rd column for post stimulus spike rates. The second

%%parameter in the function is for providing the level of significance for the t-test.

APPENDIX B

PLASMID EXTRACTION PROTOCOL USING GET™ Plasmid Mini Prep kit

GET™ Plasmid Mini Prep kit isolates high quality plasmid DNA from 1-5ml E. coli cultures. The kit utilizes an enhanced DNA binding column to produce high yields of plasmid. This quick and easy protocol eliminates toxic phenol/chloroform extractions or lengthy ethanol precipitations. On completion of the protocol, the plasmid DNA is ready for restriction enzyme digestion, sequencing, subcloning and in vitro transcription. The plasmid yields are typically up to 20μg/prep.

PREPARATION BEFORE USE

a. Add 50μl LongLife™ RNase for every 10ml Cell Suspension Solution directly to the Cell Suspension Solution bottle. After addition, store Cell Suspension Solution at 4°C. This is stable for 6 months.

b. To each bottle of DNA Wash, add 80ml molecular grade ethanol. Chill the DNA Wash to -20°C before use.

c. Chill the Neutralizing Buffer on ice prior to use, DO NOT STORE AT 4°C.

d. Warm the TE Buffer to 55-60°C before use.

PROTOCOL

1. Harvest the bacterial cells from 1-5ml overnight culture by centrifugation at >7,000x g for 3-5 minutes. Discard the supernatant.

2. Ensure that the LongLife™ RNase was added into the Cell Suspension Solution. Add 250μl Cell Suspension Solution to the bacterial pellet and re-suspend.

3. Add 250μl Lysis Buffer. Mix gently by inverting the tube until the lysate is clear, do not vortex. To ensure complete RNA digestion, incubate the tube for 2-5 minutes at room temperature. Do not exceed a 5 minute incubation and do not vortex.

4. Add 350μl chilled Neutralizing Buffer and gently invert 8-10 times to mix. Lysate should contain a thick white precipitate.

5. Centrifuge for 15 minutes at 15,000x g.

6. Ensure the GET™ Plasmid Mini column is in a collection tube and apply the supernatant on to the column. Centrifuge for 30-60 seconds at maximum speed and discard the flow through.

7. Wash the column by adding 500μl DNA Wash and centrifuge for 30-60 seconds at maximum speed. Discard the flow through. Repeat this step once.

8. Perform a final spin of the column for 60 seconds to remove any residual DNA Wash from the sides of the column.

   NOTE: We recommend placing the columns at 37-55°C for 10-30 minutes to ensure all residual alcohol is removed. This helps eliminate issues with the residual alcohol, including samples leaving agarose gel wells during loading.

9. Place the column in a clean 1.5ml tube. Elute the plasmid DNA from the column by adding 50µl pre-warmed TE Buffer directly to the column membrane. Incubate for 1-2 minutes at room temperature and then centrifuge for 30-60 seconds. The eluted plasmid is ready for restriction digestion, sequencing and other downstream applications.

BIOGRAPHICAL SKETCH

Ankur Shah, is a Biomedical Engineer currently pursuing Master''s in Science at Arizona State University. As an enthusiastic and a self-motivated person, he likes learning new skills and solving problems at the interface of Biology and Engineering. He earned his Bachelor's in Biomedical Engineering from Gujarat Technological University, India. After a brief stint with a fitness product start-up, he moved to ASU for graduate studies. Currently at Dr. Jitendran Muthuswamy's Neural Microsystems Lab, he has been looking into Novel Organic Light Emitting Diodes for Optogenetic Stimulation of Neurons. He has tested Organic Light Emitting Diodes in both invitro as well as invivo animal models. He wishes to continue his educational journey by pursuing a PhD at the University of Utah. His next research shall be in design of low energy Implantable Cardiac Defibrillation strategies.